UNIVERSITATEA NAȚIONALĂ DE ŞTIINŢĂ ŞI TEHNOLOGIE POLITEHNICA BUCUREȘTI

Școala doctorală INGINERIE MECANICĂ ȘI MECATRONICĂ

TEZĂ DE DOCTORAT

(rezumat extins– limba engleză)

Autor: Drd. ing. dipl. **GHEORGHE-COSMIN CIOCOIU**

Conducător de doctorat: Prof. univ. emerit dr. ing. **RADU I. IATAN**

București 2024

UNIVERSITATEA NATIONALĂ DE ŞTIINŢĂ ŞI TEHNOLOGIE POLITEHNICA BUCUREŞTI

Facultatea: INGINERIE MECANICĂ ŞI MECATRONICĂ
Departament: ECHIPAMENTE PENTRU PROCESE INDUSTRIALE
Școala doctorală: INGINERIE MECANICĂ ŞI MECATRONICĂ

TEZĂ DE DOCTORAT

”*CERCETĂRI TEORETICE ŞI EXPERIMENTALE PRIVIND EVALUAREA STĂRILOR DE TENSIUNI ÎN ZONELE CU DISCONTINUITĂŢI GEOMETRICE ŞI/SAU DE MATERIAL ALE ECHIPAMENTELOR INDUSTRIALE SUB PRESIUNE ŞI/SAU TEMPERATURĂ*”

”*THEORETICAL AND EXPERIMENTAL RESEARCH REGARDING THE ASSESSMENT OF STRESS STATES IN AREAS WITH GEOMETRIC AND/OR MATERIAL DISCONTINUITIES OF INDUSTRIAL EQUIPMENT UNDER ORESSURE AND/OR TEMPERATURE*”

Autor: Drd. ing. dipl. CIOCOIU GHEORGHE - COSMIN
Conducător științific: Prof. univ. emerit dr. ing. IATAN I. RADU

Comisia de doctorat

Preşedinte	**Prof. univ. abil. dr. ing. IONEL PÎŞĂ**	**de la**	**Universitatea Naţională de Ştiinţă şi Tehnologie POLITEHNICA Bucureşti**
Conducător de doctorat	**Prof. univ. emerit dr. ing. RADU I. IATAN**	**de la**	**Universitatea Naţională de Ştiinţă şi Tehnologie POLITEHNICA Bucureşti**
Referent	**Prof. univ. dr. ing. LUMINIŢA BIBIRE**	**de la**	**Universitatea “VASILE ALECSANDRI” din Bacău**
Referent	**Prof. univ. dr. ing. ANDREI DUMITRESCU**	**de la**	**Universitatea PETROL – GAZE din Ploieşti**
Referent	**Conf. univ. dr. ing. NICOLETA SPOREA**	**de la**	**Universitatea Naţională de Ştiinţă şi Tehnologie POLITEHNICA Bucureşti**

BUCUREŞTI 2024

UNIVERSITATEA NAȚIONALĂ DE ŞTIINŢĂ ŞI TEHNOLOGIE POLITEHNICA BUCUREȘTI

Școala doctorală INGINERIE MECANICĂ ȘI MECATRONICĂ

TEZĂ DE DOCTORAT

”*CERCETĂRI TEORETICE ŞI EXPERIMENTALE PRIVIND EVALUAREA STĂRILOR DE TENSIUNI ÎN ZONELE CU DISCONTINUITĂŢI GEOMETRICE ŞI/SAU DE MATERIAL ALE ECHIPAMENTELOR INDUSTRIALE SUB PRESIUNE ŞI/SAU TEMPERATURĂ*”

”*THEORETICAL AND EXPERIMENTAL RESEARCH REGARDING THE ASSESSMENT OF STRESS STATES IN AREAS WITH GEOMETRIC AND/OR MATERIAL DISCONTINUITIES OF INDUSTRIAL EQUIPMENT UNDER ORESSURE AND/OR TEMPERATURE*”

Conducător de doctorat: **Prof. univ. emerit dr. ing. RADU I. IATAN**

Doctorand: **ing. dipl. GHEORGHE-COSMIN CIOCOIU**

București 2024

UNIVERSITATEA NAȚIONALĂ DE ŞTIINŢĂ ŞI TEHNOLOGIE POLITEHNICA BUCUREȘTI

Școala doctorală INGINERIE MECANICĂ ȘI MECATRONICĂ

TEZĂ DE DOCTORAT

(Summary in English)

C H A P T E R 1

GENERAL ASPECTS REGARDING THE TYPES OF SHAPE DEVIATIONS, SURFACE DEFECTS AND GEOMETRIC STRUCTURAL DISCONTINUITIES IN THE CASE OF TECHNOLOGICAL EQUIPMENT UNDER PRESSURE. DEVELOPED INFLUENCES ON THE BEARING CAPACITY

1. 1. Introduction

The present study aims to provide information on the stress states in areas with shape deviations and geometric structure discontinuities of industrial pressure equipment, intended for use in industrial processes, which may have practical implications for the design, use and maintenance of equipment, in order to operate safely throughout the service life.

Knowledge of residual/residual stresses can help predict the behavior and performance of pressure equipment under different load conditions, which is crucial for ensuring its structural integrity.

The bearing capacity and service life of industrial process equipment play an important role, the results obtained from the analysis of stress states having a high level of confidence and being particularly useful for gaining experience and establishing practical criteria for the selection of repair procedures for the purpose of safe operation.

Fig. 1. 1. Road transport of oversized equipment
[https://www.observatordearges.ro/transporturi-agabaritice-in-arges-7.html]

1. 2. Aspects regarding the transport of oversized industrial equipment

The transport of various industrial substances is a very acute problem worldwide. To solve this problem, different methods were used for transportation:

- auto transport **[1, 2]**, – **figure 1. 1** – **figure 1. 4;**

- Rail transport **[3] - figure 1. 5.**

Some damage, due to excessive deformation, for example, can occur when transporting equipment, especially oversized equipment, on railway platforms or on platforms with tires **[108]**.

Fig. 1. 2. Road transport of oversized equipment
[https://arges-stiri.ro/2018/07/26/arges-transport-agabaritic/]

Fig. 1. 3. Road transport of oversized equipment
[https://trans.info/ro/sfaturi-utile-pentru-transportul-agabaritic-70757]

Fig. 1. 4. Fluid transport tank
[https://www.holdingredlich.com/dangerous-goods-in-the-transport-supply-chain]

1. 3. Corrosion of pipes

Particular care is taken with gas mains **[4] – Figure 1. 6**. This method is currently the most accepted, due to its cost-effectiveness, which can be attributed to the following advantages: a) high speed of delivery to facilities and storage points; b) wide geographical coverage; c) transporting the product over long distances; d) ensuring uninterrupted deliveries regardless of climatic conditions; e) minimal loss of resources during transit.

However, there are also emergency risks during the transport of fluids through pipelines, for various reasons: a) corrosion of the pipeline material **(fig. 1. 7; 1. 8; 1. 9);** b) the concentration of stresses along the structural elements; c) structural defects [**5 - 9] - Figure 1. 10**; d) external impacts on structural parts **[10 - 14]** which, as a result of the impact of internal pressure, are subject to destruction **[15 - 18]** and lead to accidents **[19 - 22]**.

The investigation of the problem of the destruction of main and conventional gas pipelines has been the basis for the adoption of a multitude of design norms and codes **[23 -30].** In 1970, the problem of cracks along pipes and ways to stop them was studied **[31].** In 1980, large-scale investigations were carried out on the rupture of large-diameter pipes, where the emphasis was placed on the method of manufacture and mechanics of the pipe material **[32, 33].** In studies conducted in 1990 **[34, 35],** the problem of the propagation of the main cracks, which is induced by the movement of the gas, was established.

The development of a calculation program, which consists of three modules, has been described: stress state analysis, fluid dynamics and crack modeling. Approaches for preventing rapid crack movements were discussed. Especially at ***Melenk J. M.*** and ***Babuska I.*** **[36]** and ***Moes N. et al.*** **[37]** The extended, finite element method was used to model the state of near-crack stresses which in turn demonstrated its accuracy and reliability of assessment.

Methods to stop the development of main cracks along gas pipelines have been proposed. Authors ***Di Biagio M. et al.*** **[46]** illustrated the research experience of the European Research Group on Gas Pipeline Strength. Approaches for the analysis of plastic fracture strength have been described. Specifically, a plastic fracture model was generated, based on a numerical analysis of the stress state.

1. 4. General aspects of surface defects in the case of technological equipment under pressure

Surface defects can be: a) fine cracks (observable only on non-oxidized surfaces); b) films, scales, chips; c) surface inequalities; d) surface damage, etc.

In the current sense, the defect is the imperfection that exceeds the quantity allowed in the prescribed quality class, established by standards, technical prescriptions, etc.

Defects, under certain conditions, can reduce fatigue resistance and thus cause premature breakage of the mechanical structure. The effect of such a premature break can be, in addition to the enormous costs involved, pollution of the external environment. This is the case, for example, of pipelines for the transport of oil or natural gas, which may contain defects both in manufacture and in assembly or operation **[107].**

Lifelong management of underground pipelines is mandatory for safe hydrocarbon transmission and distribution systems. Reliability analysis is recognized as a powerful decision-making tool for risk-based design and maintenance. Both residual stresses generated during the manufacturing process and corrosion in operation reduce the ability to withstand internal and external stresses **[159].**

1. 5. General aspects of the types of form deviations in the case of technological equipment under pressure

Any part can have, as a result of manufacturing, imperfections regarding the shape of cylindrical or complex surfaces, but also the realization of contours, straight edges or with a certain complicated shape.

The deviations in the shape of the surfaces that can be found on the components of the mechanical structures under pressure, regardless of their geometry, can be deviations from: a) the given shape of the surface – **figure 1. 13; figure 1. 14**; b) circularity – **figure 1.15**; c) cylindricity **[103 - 105] – figure 1. 15;** d) given shape of the profile **[106] – figure 1. 14**; e) rectilinear – **figure 1. 16;** f) flatness **– figure 1. 17.**

1. 6. Objectives of the thesis

a) General aspects regarding the activities that ensure the reliability of an industrial equipment, following the entire route of implementation: design, manufacture, transport from supplier to beneficiary, assembly and operation itself. Obviously, an important role is played by the revisions scheduled on scientific bases.

b) Literature study on the quantification of the types of defects that may occur and the intensity produced on the load-bearing capacity of the analyzed structure.

c) Variants for evaluating the stress states in case of shape deviations and structural discontinuities existing in pressure equipment – literature study.

d) Own analytical methods for evaluating the stress states in the case of geometric discontinuities existing in the structure of the technological equipment under pressure.

e) Experimental analysis of the stress states in the areas with structural discontinuities of the technological equipment, using the electrotensometric method (resistive tensometry).

f) Analysis of stress states in areas with geometric discontinuities of technological equipment, using the finite element method.

g) Conclusions. Own contributions. Perspectives.

CHAPTER 2

VARIANTS FOR THE EVALUATION OF STRESS STATES IN CASE OF SHAPE DEVIATIONS AND STRUCTURAL DISCONTINUITIES EXISTING IN PRESSURE EQUIPMENTS.
Literature study

2. 1. Introduction

With the development of humanity, the necessities of its life have also increased. It is extremely visible the increasingly careful use of primary materials, but also of those produced later, through appropriate combinations. The goal of quantitative, qualitative and value savings is worth following. It is an essential reason taken into account in the research, design, manufacture and practical use of complex equipment in the process industries. The "*minimization*" of the consumption of construction material has a quantitative advantage, but also an economic one.

As long as it is a question of the *purely static* operation of pressure vessels, there is no objection to this reasoning – under the conditions of careful manufacture in the ordinary sense of the word. In many cases, however, pressure vessels operate in a "fatigue mode at *a low number of load cycles*", or/and at low or high temperatures, when stress concentrations and, therefore, local peaks of relative deformations have negative effects, **[2, p. 129].** As is well known, deviations of form lead to such concentrations of stresses **[3, 4].** Therefore, it is necessary to analyze these effects and to evaluate the level to which the additional stresses reach, tending to include them in the design calculations.

2. 2. Influence of form deviations

2. 2. 1. Effect of shape deviations on the strength of the construction elements of pressure vessels

2. 2. 1. 1. Deviations from the circularity of the cylindrical ferrule

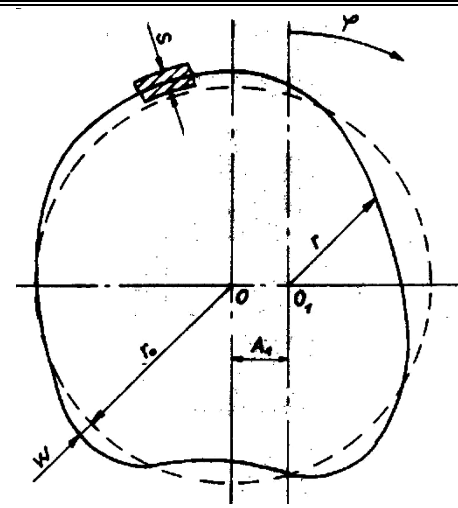

Fig. 2. 1. Schematic representation of the deformed cylindrical ferrule and the correct geometric ferrule **[6, 45]**
O_1 – the point where the current radius measuring compass joint is located r;
O – center of circumference radius r_0 ; A_1 – distance between points O şi O_1

In the construction of a technological equipment, the cylindrical ferrule is the basic element that is sometimes affected by deviations from the ***circularity of the section***, in the form of **[1, 5, 6, 45]**:

$$r^* = r_0 + \sum_{n=1}^{\infty} w_n \cdot cos\left(n \cdot \varphi + \varepsilon_n\right), \qquad (2.\ 1)$$

where : r and r_0, according to figure 2. 1; sizes w_n şi ε_n results from the calculation, when the values are known $r = r(\varphi)$, determined by measurement.

2. 2. 1. 2. Cylindrical ferrule subjected to internal pressure

In this case, apart from the ring voltages $\sigma_{2c}^{(p)} = p \cdot D_m / (2\, s)$ developed by the internal pressure p, taken into account in the design $^{**)}$, considering the geometric cylinder perfect, with the diameter D_m of the median surface, the bending ring stresses are additionally **[5, 6]**:

$$\sigma_{2c}^{(înc)} = 6\, p \cdot \frac{r_0}{s^2} \cdot \sum_{n=2}^{\infty} K_n \cdot w_n \cdot \cos\left(n \cdot \phi + \varepsilon_n\right). \qquad (2.\ 2)$$

For the cylinder subjected to external pressure, the maximum permissible deviations from the circular shape are provided for by the requirements indicated in **[1],** depending on the values D_{ext} / s and L / D_{ext}.

2. 2. 1. 4. Joining two cylindrical ferrules with off-axis median surfaces

2. 2. 1. 4. 1. The effect of the weld seam is neglected

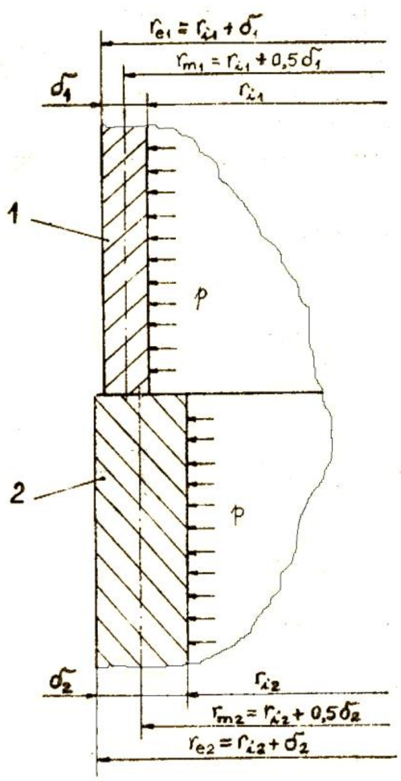

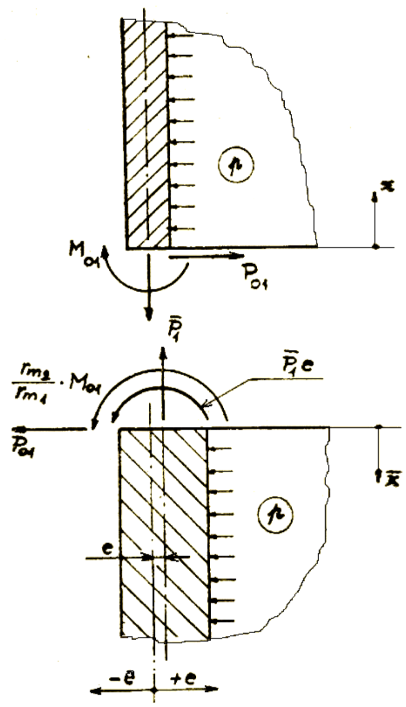

Fig. 2. 4. Joint diagram **Fig. 2. 5.** Separation of construction elements

Accepting the simplifying calculation assumptions in the field of rotational shells, and taking into account Figure 2. 4, in order to evaluate the stress and strain states in the area of junction of the two ferrules 1 and 2, it is necessary to establish, first of all, the values of the bonding loads P_{01} and M_{01} Figure 2. 5. This is possible, here, by adopting the continuity of deformations – radial displacements and rotations (angular deformations).

By solving the system of equations of the connection loads, the corresponding expressions result:

$$M_{01} = \frac{a_{13} \cdot a_{22} - a_{12} \cdot a_{23}}{a_{11} \cdot a_{22} - a_{12} \cdot a_{21}}; \qquad P_{01} = \frac{a_{11} \cdot a_{23} - a_{13} \cdot a_{21}}{a_{11} \cdot a_{22} - a_{12} \cdot a_{21}}, \tag{2. 12}$$

where influencing factors are present.

Stress states

Under the action of the external and connecting loads, the following tensions develop in the two ferrules:

- *for cylindrical ferrule* 1 (fig. 2. 4):

$$\sigma_{11}(x) = \frac{p \cdot r_{m1}}{2 \cdot \delta_1} \pm \frac{6 \cdot M_{01}^{(1)}}{\delta_1^2}; \quad \sigma_{21}(x) = \frac{p \cdot r_{m1}}{\delta_1} \pm \frac{6 \cdot \nu_1 \cdot M_{01}^{(1)}}{\delta_1^2} + \frac{T^{(1)}}{\delta_1}. \qquad (2.\ 14)$$

- *for cylindrical ferrule* 2 (fig. 2. 4):

$$\sigma_{12}\left(\bar{x}\right) = \frac{p \cdot r_{m2}}{2 \cdot \delta_2} \pm \frac{6 \cdot M_{01}^{(2)}}{\delta_2^2}; \quad \sigma_{22}\left(\bar{x}\right) = \frac{p \cdot r_{m2}}{\delta_2} \pm \frac{6 \cdot \nu_2 \cdot M_{01}^{(2)}}{\delta_2^2} + \frac{T^{(2)}}{\delta_2}. \qquad (2.\ 16)$$

<u>Note:</u> In the above relations, the loads dependent on the current dimension measured along each cylinder are considered.

The equivalent stresses are calculated with relations of the form:

$$\sigma_{echj} = \left(\sigma_{1j}^2 + \sigma_{2j}^2 - \sigma_{1j} \cdot \sigma_{2i}\right)^{0,5}; \quad j = 1,\ 2, \qquad (2.\ 18)$$

according to the theory of strain energy, or

$$\bar{\sigma}_{echj} = max\left(\sigma_{1j};\ \sigma_{2j}\right), \qquad (2.\ 19)$$

according to the theory of maximum tangential stresses.

In view of the local concentration of stresses, it is possible to accept construction for which $\sigma_{echj} \leq \sigma_a$, respectively $\bar{\sigma}_{echj} \leq \sigma_a$ or, for a more efficient use of building materials, $\sigma_{echj} \leq \bar{\sigma}_a$ respectively $\bar{\sigma}_{echj} \leq \bar{\sigma}_a$.

►▼◄

The above shows the states of stresses and deformations in the area of joint of two cylindrical ferrules, between whose median surfaces there is a certain eccentricity e, considered as a deviation from the ideal geometry. In this case, the stiffening effect of the weld seam, necessary for the joining of the two mentioned construction elements, is neglected, and it will be taken into account in another analysis.

The relations obtained allow the values of the equivalent stresses to be established and their comparison with the permissible values prescribed by the designer.

2. 2. 1. 4. 2. The effect of the weld seam is not neglected

In the present case, based on the theory of unitary bending moments, rotational shells and equality of deformations, on the one hand **[13 – 15, 32 - 34]** and the method of short structural elements, on the other hand, it is proposed to evaluate the stress state in the beveled area, of passage between two cylindrical ferrules of different thicknesses (fig. 2. 8). In the present case, it is established the method of deducting the connecting loads developed under the action of external loads, considered, between ferrules and short structural elements (cylindrical shell type with a height below the length of the half-wave [**13 – 15**], on the one hand, as well as from the mentioned elements [**19, 26, 27, 29**], on the other hand. Some recognized regulations make adequate clarifications on the geometry of such a beveled area. Practice cannot always comply with such recommendations, and as such a case-specific methodology is needed.

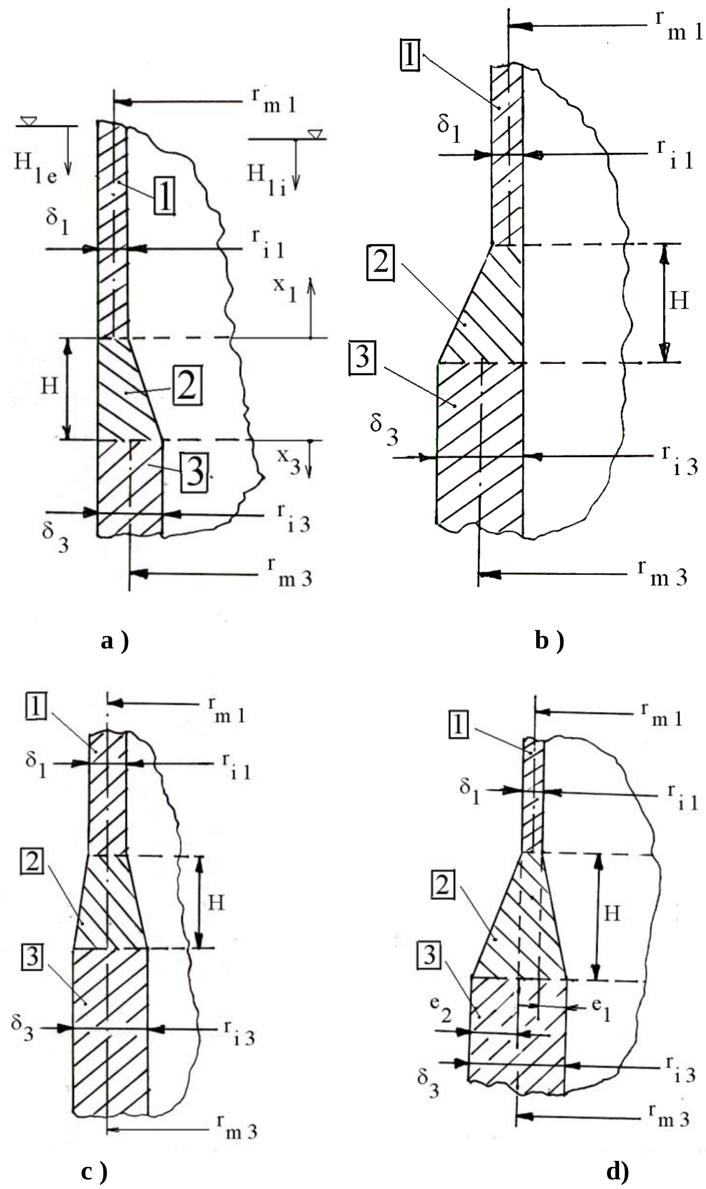

Fig. 2. 6. Types of beveled areas, connecting two successive cylindrical ferrules, with different thicknesses
a – constant external radius; b – constant inner radius; c – constant median radius (symmetrical beveled area); d – different median surfaces (non-symmetrical beveled area)

In order to achieve the proposed goal, the beveled areas (fig. 2. 6 – 2. 10), connecting the two successive cylindrical ferrules, are divided into a number of short cylindrical elements (blades).

The other geometric characteristics of the lamellar elements are established with appropriate relationships (2.23 – 2.26).

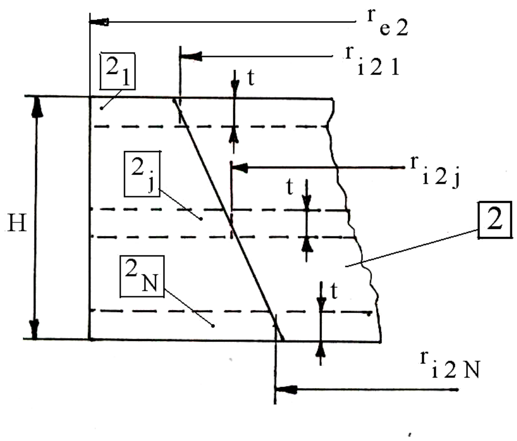

Fig. 2. 7. Dividing the beveled area by the shape in Figure 2. 6, a

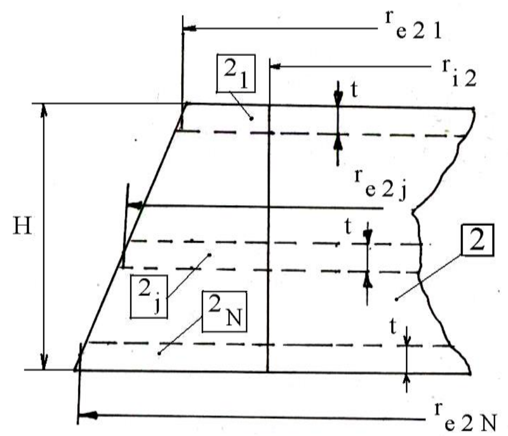

Fig. 2. 8. Dividing the beveled area of The shape in Figure 2. 6,b

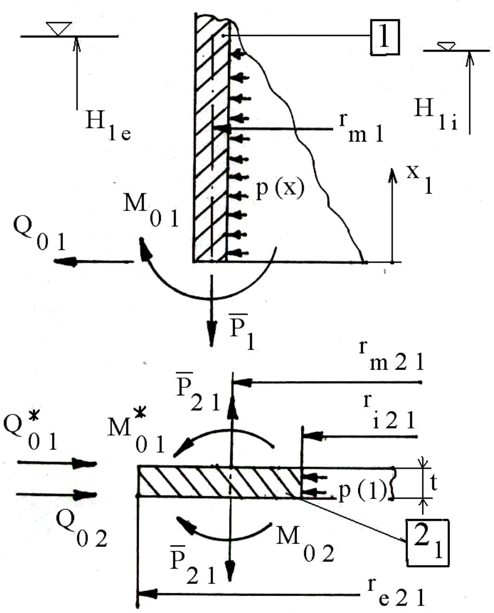

Fig. 2. 11. Scheme of separation of elements 1 and 2_1

<u>Note 1</u>: The outer radius of the cylindrical ferrules or the inner radius of the ferrule 1 (as above) or the inner radius of ferrule 3 (fig. 2. 6, a) can be taken as the basis for calculation.

<u>Note 2</u>: For the calculations that are made in the present work, the following conditions must be met:

$$\delta_1 / r_{i1} \langle \ 0,2; \quad \delta_3 / r_{i3} \langle \ 0,2, \tag{2. 27}$$

which classifies all short structural elements in the category of rotation shells **[12 – 15].**

Note 4: In the above analysis, it was considered that the structure is resting under the beveled area. When the support is above the mentioned area, the axial forces specified above must be appropriately adapted.

Continuity/compatibility equations of deformations

The figures are discussed 2. 11… 2. 13.

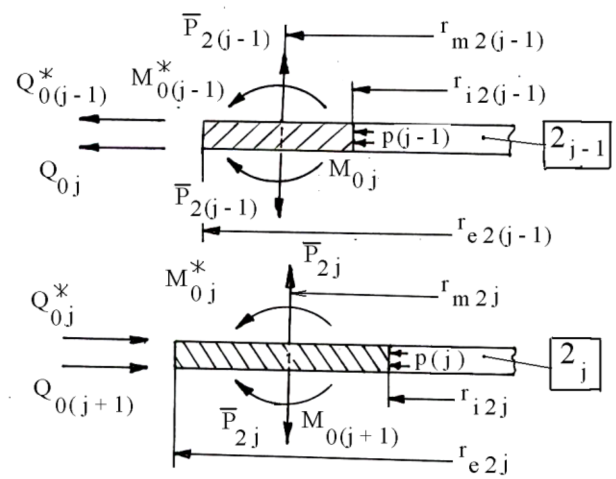

Fig. 2. 12. Scheme of separation of short structural elements 2_j and 2_{j+1}

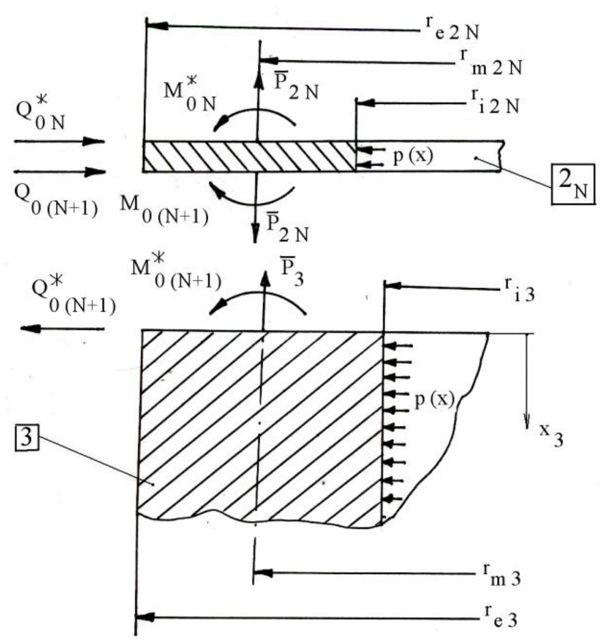

Fig. 2. 13. Diagram of separation of elements 2_N and 3

Write the equations of continuity of the deformations, according to the relations (2.35) --- (2.40) and deduce the connection loads between the lamellar elements:

► $\left\{\mathbb{N}\right\}^T = \left\{M_{01}, Q_{01}, M_{02}, Q_{02}, \cdots, M_{0j}, Q_{0j}, \cdots, M_{0(N+1)}, Q_{0(N+1)}\right\}$ - the transposed vector of the unknowns of the current problem – bonding charges – radial, unitary bending moment, and unitary shear forces. The expressions of radial and annular stresses, respectively the equivalent stresses, are further established.

►▼◄

The above presents an original methodology, based on the theory of unitary bending moments, characteristic of rotational shells, respectively the theory of short structural elements. In this sense, the aim is to determine the connection loads – radial, unitary bending moments – and unitary shear forces, existing in the planes of separation of the elements of the structure with transition areas from one thickness to another, with linear variation (the four cases analyzed). Their values can be used, in subsequent works, to evaluate the radial and annular stresses, respectively the maximum equivalent voltage. Based on its value, it can be concluded whether the structure is suitable for the given functioning, or specific adaptations can be made: changing the construction material or geometry used in the study.

2. 2. 1. 5. Shape deviations of the domed lids of the vessels

Together with the cylindrical ferrule, the domed bottom is a basic element in the construction of pressure vessels. In our country, bottoms with an elliptical profile, with an arrow profile $h_m = D_m / 4$, i.e. having a semi-axis ratio equal to 2, are used. In its central part, the elliptical profile, having the indicated geometric characteristics, can be approximated by the spherical profile, the radius being $r_e = 2 \cdot R_m$, $D_m = 2 \cdot R_m$ the diameter of the median surface of the cylindrical body that connects to the elliptical profile.

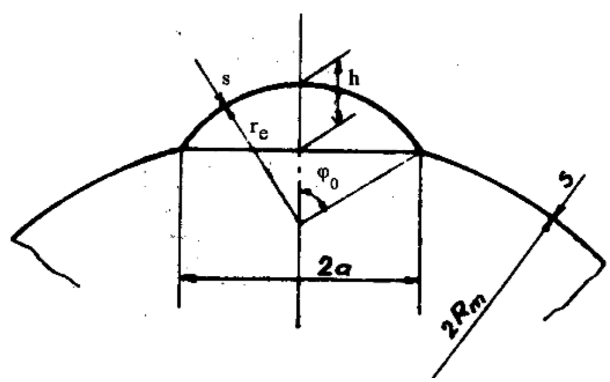

Fig. 2. 14. Spherical sheath with spherical protrusion

In some cases, there are also hemispherical caps – according to the requirements of the technological process used by the equipment – as well as conical and truncated conical caps/bottoms. In the following, the spherical casing will be examined from the point of view of manufacturing precision.

2. 2. 1. 5. 1. Spherical shell subjected to internal pressure

It can be easily ascertained, admitting that $(h/a) \langle\langle 1$, deci $(\phi/2) \approx (h/a)$.

On the contour of the protrusion embedding, the spherical sheath with radius $2 \cdot R_m$ is therefore stressed by the stresses:

$$\sigma_{1s} = \sigma_{1s}^{(ref)} + \sigma_{1s}^{(înc)} ; \quad \sigma_{2s} = \sigma_{2s}^{(ref)} + \sigma_{2s}^{(înc)} , \tag{2. 88}$$

in other words:

$$\sigma_{2s} = \left[1 \mp \frac{3 \cdot (1-\mu)}{\sqrt{3 \cdot \left(1-\mu^2\right)}} \cdot \frac{r_e}{2 \cdot R_m} \right] \cdot \frac{p \cdot R_m}{s} ; \; \sigma_{1s} = \left[1 \mp \frac{3 \cdot \mu \cdot (1-\mu)}{\sqrt{3 \cdot \left(1-\mu^2\right)}} \cdot \frac{r_e}{2 \cdot R_m} \right] \cdot \frac{p \cdot R_m}{s} . \tag{2. 89}$$

Consequently:

$$\alpha_{k,1,s} = \frac{\sigma_{1s}}{\sigma_{1s}^{(ref)}} = 1 + \frac{3 \cdot \mu \cdot (1 - \mu)}{\sqrt{3 \cdot \left(1 - \mu^2\right)}} \cdot \frac{r_e}{2 \cdot R_m} ; \; \alpha_{k,2,s} = \frac{\sigma_{2s}}{\sigma_{2s}^{(ref)}} = 1 + \frac{3 \cdot (1 - \mu)}{\sqrt{3 \cdot \left(1 - \mu^2\right)}} \cdot \frac{r_e}{2 \cdot R_m} , \tag{2. 99}$$

the highest values α_k being those of the inner surface (extent), as they result from the relations (2. 99), in which the "minus" signs of the relations (2. 89) have not been introduced.

The coefficient of stress concentration, equivalent, in relation to the equivalent stress $\sigma_{1s}^{(ref)} = \sigma_{2s}^{(ref)} = \sigma_{ech,s}^{(ref)}$ has the value:

$$\alpha_{k,ech,s} = \sqrt{\alpha_{k,1,s}^2 + \alpha_{k,2,s}^2 - \alpha_{k,1,s} \cdot \alpha_{k,2,s}} . \tag{2. 100}$$

2. 2. 1. 5. 2. Spherical shell subject to external pressure

For spherical shape, with deviations from the correct shape **[44]**:

$$p_{cr,2} = 0,365 \cdot E \cdot \left(s / R_m \right)^2 . \tag{2. 102}$$

Experience has shown that in the domain of thin-walled spheres, the relation (2.102) no longer corresponds. In general, an experimentally determined coefficient should be inserted into the formula instead of the constant coefficient $K = K\left(s / R_m\right),$. The expression is also proposed:

$$K = 2 \Big/ \left[7,5 + 0,006 \cdot \left(R_m / s \right) \right] . \tag{2. 103}$$

In the literature, even higher values are indicated for the numerical coefficient in the relation (2. 102), for example $0,457$.

What has been shown regarding the behavior of the domed bottom, respectively of the spherical shell subjected to external pressure, highlights, once again, the great importance of the quality of the manufacture.

2. 2. 1. 6. Lifetime assessment issues

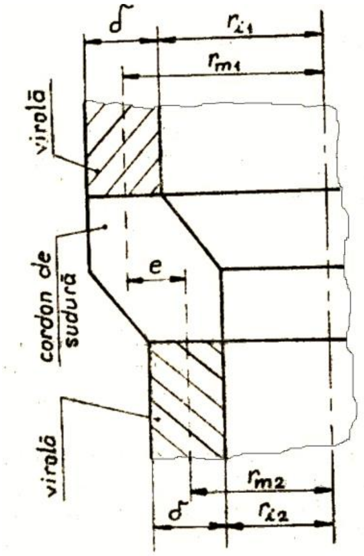

Fig. 2. 16. Deviations from the straightness of the generator

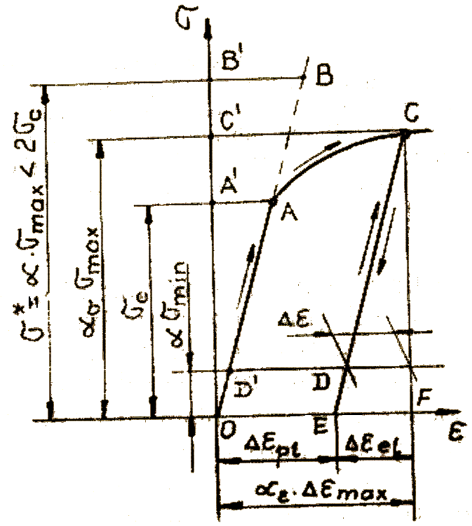

Fig. 2. 17. Plastic deformations

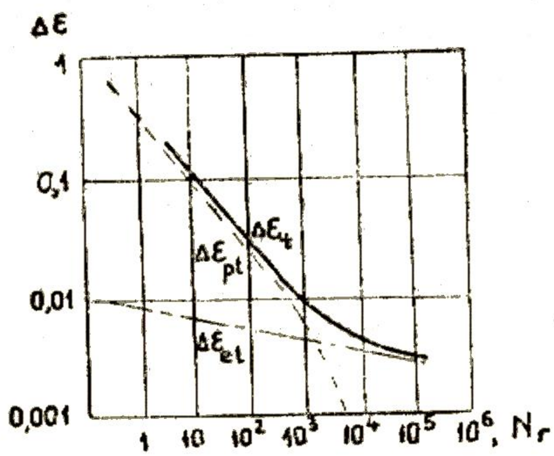

Fig. 2. 18. Number of cycles to break

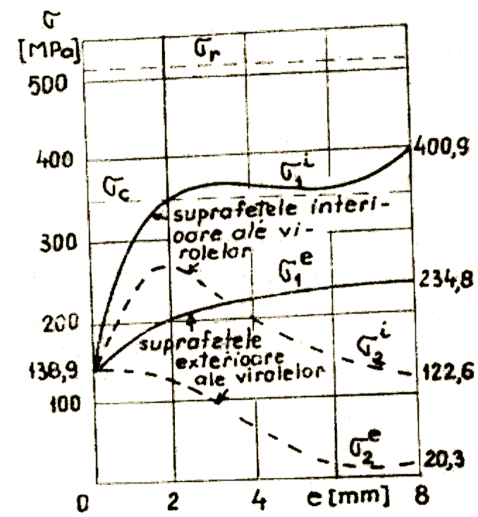

Fig. 2. 19. Stress values for the case study

In addition to the conditions for the correct choice of construction material, construction solutions and the right technology for manufacturing, avoiding geometric deviations from the correct shape in the production of pressure vessels plays a particularly important role.

The cylindrical body, the basic element in the construction of containers, is obtained by welding several ferrules together. This operation, in most cases, registers deviations from the straightness of the generator (**fig. 2. 16**). As a consequence of this imperfection of the cylindrical body realization, there appear in the area of the joint southern bending moments that lead to coefficients of concentration of the stresses with important values.

In the works **[36, 37]** the case of two cylindrical ferrules with offset median surfaces with an eccentricity "e" was analyzed, stressed by a constant internal pressure. In the present study, the durability of the same welded joint is studied, in the case of pulsating internal pressure stress or, in other words, the joint is studied at oligocyclic fatigue (fatigue at less than 10^{5} load cycles). The phenomenon is conditioned by the plastic deformations that occur during the operation of the containers.

The relationship between the amplitude of the total deformation, $\Delta\varepsilon_i$, of the plastic deformation, $\Delta\varepsilon_e$, and the number of cycles until rupture (N_r), is represented in **figure 2. 18 [38]**. As the calculus relation for its determination N_r, the ***Mannson-Coffin*** relation is chosen **[39]**:

$$\Delta\varepsilon_t = \frac{3{,}5\cdot\sigma_r^T}{E^T\cdot N_r^{0{,}12}} + \left(\frac{ln\dfrac{100}{100-\psi_r}}{N_r}\right)^{0{,}6}, \qquad (2.\ 106)$$

where: $\Delta\varepsilon_t$ - the amplitude of the total deformation occurring in the area of the joint, [%]; σ_r^T - the tear strength of the material at the working temperature, [N /m ^{2}]; E^T - modulus of elasticity of the material, at the design temperature, [N/m2]; ψ_r - neck at breakage, [%].

For the application of the relation (2. 106) it is necessary to determine the amplitude of the total deformation, $\Delta\varepsilon_t$, knowing the stresses that develop in the case studied (fig. 2. 19).

Case I

For the four situations e = 2, 4, 6 and 8 mm, $\sigma_{max} \rangle \sigma_c$ (but $\sigma_{max} \langle\ 2\cdot\alpha_c$), the coefficient of concentration of the stresses in the elastic range is determined:

$$\alpha = \sigma_{max} / \sigma_{membrană}, \qquad (2.\ 107)$$

and the stress concentration coefficient $\alpha_k(\sigma)$ in the plastic stress field:

$$\alpha_k(\sigma) = \sigma_{max}/\sigma_c. \qquad (2.\ 108)$$

Applying the ***Neuber*** relationship***:***

$$\alpha_k^2 = \alpha_k(\sigma)\cdot\alpha_k(\varepsilon), \qquad (2.\ 109)$$

the coefficient of concentration of deformations in the plastic field is determined:

$$a_k(\varepsilon) = \alpha_k^2 / [\alpha_k(\sigma)]. \qquad (2.\ 110)$$

Knowing on $\alpha_k(\varepsilon)$, we can calculate the amplitude of the plastic deformation that occurred in each case:

$$\Delta\varepsilon_{pl} = \Delta\varepsilon_c \cdot [\alpha_k(\varepsilon) - 1]. \qquad (2.\ 111)$$

relationship in which:

$$\Delta\varepsilon_c = \Delta\sigma_c / \mathrm{E}.. \qquad (2.\ 112)$$

The amplitude of the total deformation is determined by the relation:

$$\Delta\varepsilon_t = \Delta\,\varepsilon_{p\,l} + \Delta\varepsilon_{el}\,. \tag{2. 113}$$

Note: In the continuation of the study, two other cases are considered.

►▼◄

Following the calculations carried out, the following can be found:

a) the durability of the joint (the number of cycles until breakage Nr) decreases by half when the eccentricity of the ferrules increases from e = 2 mm to e = 8 mm;

b) The differences between the results obtained, applying the three calculation modes, are large in the field of small eccentricities and decrease greatly in the field of large eccentricities;

c) The curves allow the direct determination of its values N_r for eccentricities between 2 - 8 mm.

2. 2. 1. 6. 2. Technological pipelines, Case study.

* * *

The study, taking into account the stress states developed in a pipe section, for minimum measured thicknesses, after 18 years of operation and 17 years of conservation, under the action of regime pressure and test pressure, proposes a subsequent period of 12 years of operation. The value of the residual life is established based on the criterion of thinning the wall, with an average corrosion rate corresponding to the previous 35 years, and ensuring the resistance conditions.

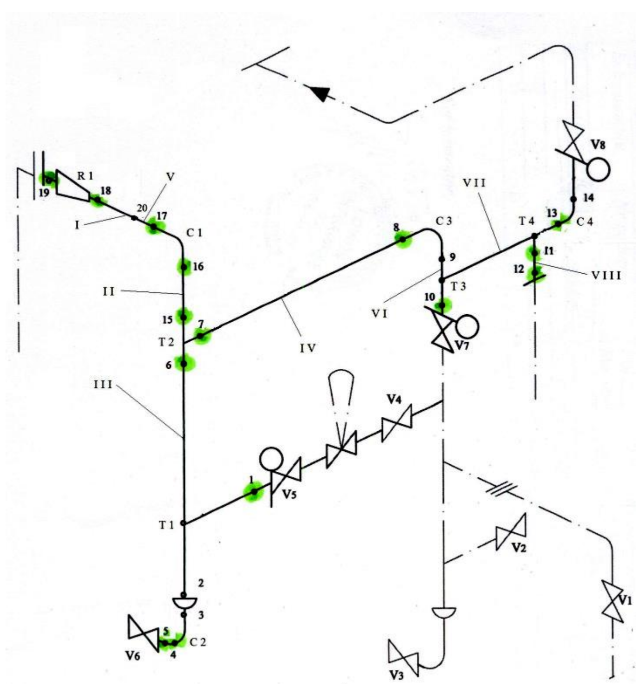

Fig. 2. 21. Pipeline section - diagram

* * *

The problem of extending the service life of some industrial components, after the end of the forecast interval, on the one hand, but also after being out of service for a period of time, on the other hand, is an interesting, exciting, but also difficult one.

The present analysis discusses a section of pipeline that is part of a petrochemical plant.

2. 2. 1. 6. 2. 3. Pipeline section $\varnothing\, 273 \times 9,3$

Evaluation of the residual service life

If the simplified durability diagram and the nominal stress process **[50, 51] are** adopted, a very large number of cycles (considering a pulsating cycle) is established, i.e. a practically indeterminate state. Looking for a duration of limited value, the principle of progressive thinning of the wall is chosen in the following.

In this regard, the average corrosion rate during the 35 years since the commissioning of the plant is taken into account, of which 18 years of normal operation and 17 years of conservation: $v_c = 0,031\, mm / year$.

By entering the known data, the permissible thinning is determined $a = 5,05\, mm$. Reaching this value of the depth of the defect considered, under the conditions of maintaining the corrosion rate calculated above, leads to a period of over 57 years.

Adopting a residual service life of 12 years, as in the case of machinery with which the pipe is connected, the thinning of the wall would be equal to: $\Delta s = 0,031 \cdot 12 = 0,37\ mm$, which added to the current condition leads to a defect depth of: $\Delta s_{12} = 1,1 + 0,37 = 1,47\ mm$.

The resistance thickness, after the 12 years of subsequent use, is 9.3 – 1.47 = 7.83 mm, when the average radius is $131,1\, mm$.

The maximum equivalent voltage, after the next 12 years, has the value:

$$\sigma_{ech}^{III} = \frac{2,5 \cdot 131,1}{7,83} = 42,0\ N / mm^2 \ \langle\ 76\ N / mm^2 \text{ sau } 64,6\ N / mm^2 .$$

The resistance condition, according to item 2.6.1.2 **[49],** is met, the subsequent period of use of the pipe being justified.

In hydraulic testing, the maximum equivalent voltage has the value:

$$\sigma_{ech}^{III} = 62,0\ N / mm^2 \ \langle\ 207\ N / mm^2 ,$$

the condition of resistance being fulfilled in this case as well.

2. 2. 1. 6. 2. 4. Pipeline section $\varnothing\, 114,3 \times 6$

The minimum (calculated) thickness of the pipe wall has the value: $s_c = 2,16\ mm \ \langle\ 6,0\ mm$.

The measured thickness is 5.2 mm (in the characteristic area of the C3 elbow). The average range is: $r_m = 53,75\,mm$.

Design pressure $\left(p_c = 2,5\,MPa\right)$; **Hydraulic Test Pressure** $\left(p_h = 3,7\,MPa\right)$

The stenght condition is met.

.

2. 2. 1. 6. 2. 5. Pipeline section $\varnothing\ 26,7 \times 2,9$

The minimum (calculated) resistance thickness of the pipe wall is: $s_c = 0,51\ mm \langle\ 2,9\ mm$.

The measured thickness is 3.2 mm (section VIII – fig. 1).

The average radius has the value: $r_m = 12,05\,mm$.

Design pressure $\left(p_c = 2,5\,MPa\right)$. Endurance condition 2.6.1.2 **[49]** is met.

Hydraulic test pressure $\left(p_h = 4,0MPa\right)$. The resistance condition is met.

2. 2. 1. 6. 2. 6. Stresses in bends

Estimating the service life

In order to estimate the subsequent life of the bends, it is noted that the corrosion speed is lower than the one estimated on the linear area of the pipe (taking into account the C4 bend): $v_c = 0,023\,mm\,/\,year$, representing 74% of the value of the corrosion speed on the right portion of the pipe.

Proposing a ***future operation of 12 years***, there is a decrease in the wall thickness (corresponding to the C4 elbow) by the value $0,023 \cdot 12 = 0,28\,mm$, which would lead to the wall thickness on the inside of the elbow equal to $9,1 - 0,28 = 8,82\,mm = s_i^{\bullet}$, and on the outside of it $9,0 - 0,28 = 8,72\,mm = s_e^{\bullet}$. With these data, it is further determined $d_e^{\bullet} = 271,84\,mm$; $R_e^{\bullet} = 407,76\,mm$.

The values of the established voltages show that the service life for the pipeline is viable. The conditions of resistance in both cases are met.

2. 2. 1. 6. 2. 7. Conclusions and recommendations

- The exposed calculation brief established first of all the minimum resistance thicknesses necessary for acceptance for the design of the analyzed pipe components, followed by the analysis of the stress states created in the places where thickness measurements were made with the help of ultrasound.

- The stress states calculated in the different areas of the pipe route, where decreases in the wall thickness have been found, meet the resistance conditions required by the regulations in force, both for the calculation and for the hydraulic testing pressure.

- Taking into account the process of progressive thinning of the pipe wall, with corrosion rates similar to those deduced for the period of existence of the pipe (including both normal operation – 18 years – and conservation – 17 years), it is proposed to use this structure for another

12 years. Obviously, at this stage the legal examinations will be carried out and the necessary conclusions will be adopted.

CHAPTER 3

OWN ANALYTICAL METHODS FOR THE EVALUATION OF STRESS STATES IN THE CASE OF GEOMETRIC DISCONTINUITIES EXISTING IN THE STRUCTURE OF TECHNOLOGICAL EQUIPMENT UNDER PRESSURE

3. 1. Introduction

Chemically and/or mechanically aggressive substances can lead to damage to components, which is why theoretical, analytical and numerical methods, as well as experimental methods, must be developed for estimating current stress states. The above refers to static pressure equipment: pressure vessels with geometric discontinuities or structural imperfections, technological pipes [**1**], flange assemblies [**2 - 14],** heating/cooling jackets **[15, 16**]; dynamic equipment: centrifugal [**17, 18, 19, 20**]; criteria regarding the breakage of materials [**21**], holes, notches, for example.

3. 2. Analytical study of stress states in cylindrical areas with geometric discontinuities

This study addresses the analytical evaluation of the stress states developed in a geometric structure composed of neighboring cylindrical areas, with different geometries, with passage without connection between them – **figure 3. 1**. For the determination of the bonding loads (unitary shear forces Q_{01}, Q_{02} $[N/m]$ and unitary bending moments $M_{01}, M_{02}\,[N\cdot m/m]$) – figure 3. 2 - the compatibility of the continuity equations of radial displacements and rotations of neighboring elements shall be used.

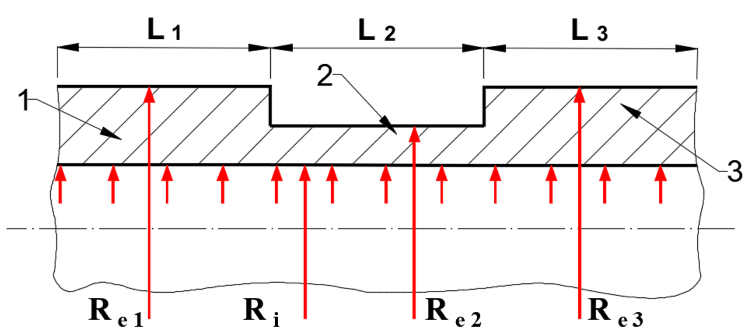

Fig. 3. 1. The geometric structure under analysis **[20]**

3. 2 . 1. Study hypotheses

1. The construction material of the cylindrical sections is considered homogeneous, isotropic and continuous. The request shall be considered in the elastic field. The transition between sections, with different thicknesses, is abrupt (without linear or curved passage).

2. The intermediate section is of constant thickness, smaller than the side sections. Its length falls into the category of short cylinders [**23**]: $L_2 < L_{sc} \approx 12.5 \cdot \sqrt{R_{m2} \cdot \delta_2}$ (length less than the length of the characteristic half-wave **[23])**

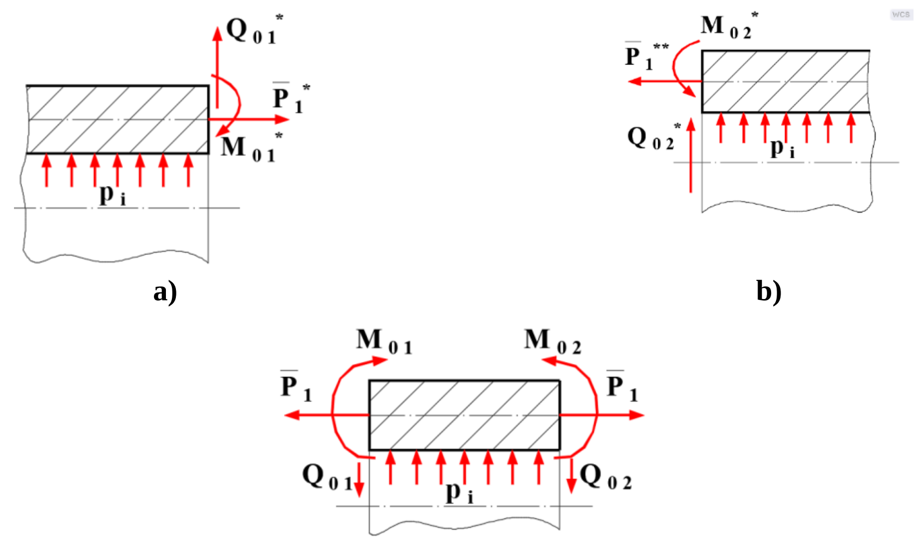

Fig. 3. 2. Discretization and loading of the analyzed geometric structure
a - Structural element 1; b) – Structural element 3; c) structural element 2 (short cylindrical element) **[20]**

3. 2. 2. Establishing binding tasks

In order to determine the connection loads of the present case, the deformation continuity equations are written, resulting in the linear algebraic system:

$$[A] \cdot \{M_{01}, Q_{01}, M_{02}, Q_{02}\}^T = \{b_1, b_2, b_3, b_4\}^T, \tag{3. 1}$$

where $[A]$ represents the null matrix of the factors influencing the bonding loads:

$$[A] = \begin{bmatrix} a_{11} & a_{12} & a_{13} & a_{14} \\ a_{21} & a_{22} & a_{23} & a_{24} \\ a_{31} & a_{32} & a_{33} & a_{34} \\ a_{41} & a_{42} & a_{43} & a_{44} \end{bmatrix}. \tag{3. 2}$$

The linked tasks, mentioned, are established using equality:

$$\{M_{01}, Q_{01}, M_{02}, Q_{02}\}^T = [A]^{-1} \cdot \{b_1, b_2, b_3, b_4\}^T, \tag{3. 6}$$

where $[A]^{-1}$ is the inverse of the non-zero matrix $[A]$.

3. 2. 3. States stress

3. 2. 3. 1. Cylindrical elements 1 and 3

The axial $\sigma_{1t}(x)$ and annular stresses $\sigma_{2t}(x)$ developed in cylindrical elements 1 and 3, under the action of external loads – internal pressure and temperature – have the expressions:

$$\sigma_{1t}(x)=\frac{p_i \cdot R_{mt}}{2\cdot\delta_t} \pm \frac{6\cdot M_{ct}(x)}{\delta_t^2} + E\cdot\alpha_T\cdot\Delta T_t; \tag{3. 8}$$

$$\sigma_{2t}(x)=\frac{p_i \cdot R_{mt}}{\delta_t} \pm \frac{6\cdot\nu\cdot M_{ct}(x)}{\delta_t^2} + \frac{T_t(x)}{\delta_t} + E\cdot\alpha_T\cdot\Delta T_t. \tag{3. 9}$$

<u>Note:</u> In the previous relations, the current sections along the cylindrical elements are considered.

3. 2. 3. 2 Cylindrical element 2

The expressions for the radial tension $\sigma_{12}(x)$ and for the annular tension $\sigma_{22}(x)$, corresponding to cylinder 2 (**fig. 3.1**), have the forms:

$$\sigma_{12}(x)=\frac{p_i \cdot R_{m2}}{2\cdot\delta_2} \pm \frac{6\cdot M_{2x}(x, M_{01}, M_{02})}{\delta_2^2} \mp \frac{6\cdot M_{2x}(x, Q_{01}, Q_{02})}{\delta_2^2} + E\cdot\alpha_T\cdot\Delta T_2; \tag{3. 13}$$

$$\sigma_{22}(x)=\frac{p_i \cdot R_{m2}}{\delta_2} \pm \frac{6\cdot K_{2x}(x, M_{01}, M_{02})}{\delta_2^2} \mp \frac{6\cdot K_{2x}(x, Q_{01}, Q_{02})}{\delta_2^2} +$$

$$+\frac{T_{2x}(x, M_{01}, M_{02})}{\delta_2} + \frac{T_{2x}(x, Q_{01}, Q_{02})}{\delta_2} + E\cdot\alpha_T\cdot\Delta T_2. \qquad (3.\ 14$$

<u>Note</u>: In the equalities (13) and (14) the plus sign for the radial unitary bending moments $M_{2x}(x, M_{01}, M_{02})$ and $K_{2x}(x, M_{01}, M_{02})$ is characteristic of the inner surface of the cylindrical element 2. In the case of radial unitary bending moments $M_{2x}(x, Q_{01}, Q_{02})$, $K_{2x}(x, Q_{01}, Q_{02})$ the plus sign also belongs to the outer surface of the short cylinder 2 (fig. 3. 2). In the case of the same ties (3. 13) and (3. 14), the annular unit forces have the plus sign for $T_{2x}(x, M_{01}, M_{02})$, respectively the minus sign for $T_{2x}(x, Q_{01}, Q_{02})$, as shown by the equalities (3. 19) and (3. 20). The dimension x has the zero origin in the separation plane of elements 1 and 2 and the maximum value ($x = L_2$), in the separation plane of components 2 and 3.

3. 2. 4. Conclusions

In the previous study, the connection between two long cylindrical elements and a short, intermediate cylindrical element is considered. The continuity equations of radial and angular deformations are established, so that based on the linear algebraic system the expressions of the bond loads are deduced – unitary bending moments and unitary shear forces. With the help of these, the expressions of radial and annular stresses (plane stress state) are described, dependent on a current dimension, expressed in context. The previous calculation methodology can also be used if the transitions from one structure to another will be with connection or linear passage.

3. 3. Analytical study of stress states in a flat circular plate and a central connection

3. 3. 1. Study hypotheses

In the structure of industrial equipment, there are often combinations between central connections for the supply of fluids (liquids or gases) and circular flat plates, joined, in turn, with cylindrical bodies.

<u>Note</u>: The experimental model adopted and specified above (**fig. 3. 1**) has a combination of the kind presented above. The calculation assumptions specific to the rotation shells are taken into account.

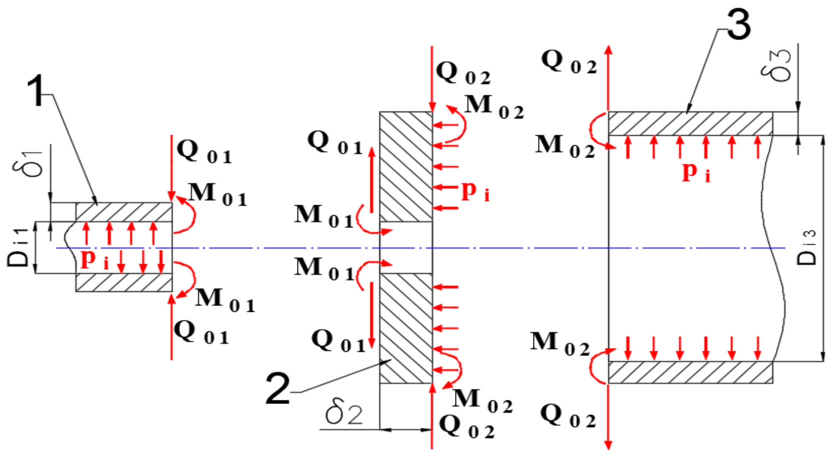

Fig. 3. 3. Diagram of separation of the elements of the joint of the central connection with a flat circular plate, fixed to a cylindrical body **[21]**

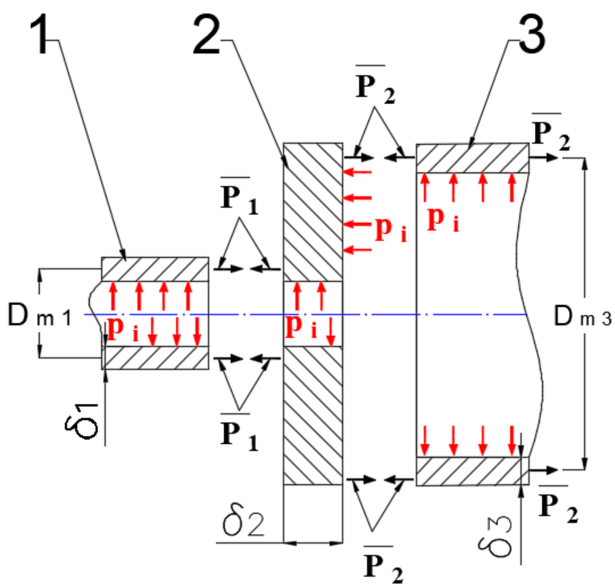

Fig. 3. 4. Diagram with the unitary axial forces $\overline{P}_1$, $\overline{P}_2$, distributed on the medial circumferences of cylinders 1 and 3 **[21]**

3. 3. 2. Deformation continuity equations. Loads connection

Writing the equations of continuity of radial deformations and rotations for elements 1 and 2, respectively 2 and 3, results in the algebraic system written in the form:

$$[A]\cdot\{S_l\}=\{T_l\}, \tag{3. 24 }$$

where the determinant *of influencing factors* takes the form:

$$[A]=\begin{bmatrix} b_{11} & b_{12} & b_{13} & b_{14} \\ b_{21} & b_{22} & b_{23} & b_{24} \\ b_{31} & b_{32} & b_{33} & b_{34} \\ b_{41} & b_{42} & b_{43} & b_{44} \end{bmatrix}. \tag{3. 25}$$

3. 3. 3. Stress states

Next, the *radial and annular stresses* are evaluated along the sections of the tube for the discharge of the separated dust, for a flat state of static stress.

The action of external loads - constant

The radial σ_1 and annular stresses σ_2 , constant along the length of the cylindrical elements 1 and 3 (fig. 3. 3), have the forms:

- ***For the cylindrical element 1*** (**fig. 3. 3**):

$$\left[(\sigma_1)_{1x}\right]_{p_i,\Delta T_1}=\left[(\sigma_1)_{1x}\right]_{p_i}+\left[(\sigma_1)_{1x}\right]_{\Delta T_1}=p_i\cdot R_{m1}\big/(2\cdot\delta_1)+E_1\cdot\alpha_1\cdot\Delta T_1\,; \tag{3. 54) 1}$$

$$\left[(\sigma_2)_{1x}\right]_{p_i,\Delta T_1}=\left[(\sigma_2)_{1x}\right]_{p_i}+\left[(\sigma_2)_{1x}\right]_{\Delta T_1}=p_i\cdot R_{m1}\big/\delta_1+E_1\cdot\alpha_1\cdot\Delta T_1\,; \tag{3. 54) 2}$$

$$\left[(\sigma_2)_{1x}\right]_{p_i}=2\cdot\left[(\sigma_1)_{1x}\right]_{p_i}\,;\ \left[(\sigma_1)_{1x}\right]_{\Delta T_1}=\left[(\sigma_2)_{1x}\right]_{\Delta T_1}=E_1\cdot\alpha_1\cdot\Delta T_1\,. \tag{3. 54) 3}$$

- ***For the cylindrical element 3*** (fig. 3. 3):

$$\left[(\sigma_1)_{3x}\right]_{p_i,\Delta T_3}=\left[(\sigma_1)_{3x}\right]_{p_i}+\left[(\sigma_1)_{3x}\right]_{\Delta T_3}=p_i\cdot R_{m3}\big/(2\cdot\delta_3)+E_3\cdot\alpha_3\cdot\Delta T_3\,; \tag{3. 55) 1}$$

$$\left[(\sigma_2)_{3x}\right]_{p_i,\Delta T_3}=\left[(\sigma_2)_{3x}\right]_{i}\left[(\sigma_2)_{3x}\right]_{\Delta T_3}=p_i\cdot R_{m3}\big/\delta_3+E_3\cdot\alpha_3\cdot\Delta T_3\,; \tag{3. 55) 2}$$

$$\left[(\sigma_2)_{3x}\right]_{p_i}=2\cdot\left[(\sigma_1)_{3x}\right]_{p_i}\,;\ \left[(\sigma_1)_{3x}\right]_{\Delta T_3}=\left[(\sigma_2)_{3x}\right]_{\Delta T_3}=E_3\cdot\alpha_3\cdot\Delta T_3\,. \tag{3. 55) 3}$$

Action of loads connection

- ***For the cylindrical element 1*** (**fig. 3. 3**):

$$\left\{(\sigma_1)_{1x};(\sigma_2)_{1x}\right\}=\left\{\left[(\sigma_1)_{1x}\right]_{p_i,\Delta T_1}\cdot\left(c_{i\sigma r}\right)_{1x};\ \left[(\sigma_2)_{1x}\right]_{p_i,\Delta T_1}\cdot\left(c_{i\sigma i}\right)_{1x}\right\}\,; \tag{3. 58) 1}$$

$$\left(c_{i\sigma r}\right)_{1x}=1+\left\{\left(\pm 6\cdot M_{1x}/\delta_1^2\right)\Big/\left[p_i\cdot R_{m1}/(2\cdot\delta_1)+E_1\cdot\alpha_1\cdot\Delta T_1\right]\right\}; \tag{3. 58) 2}$$

$$\left(c_{i\sigma i}\right)_{1x} = 1+\left\{\left[\pm 6\cdot\mu_1\cdot M_{1x}/\delta_1^2+T_{1x}/\delta_1\right]/\left[p_i\cdot R_{m1}/\delta_1+E_1\cdot\alpha_1\cdot\Delta T_1\right]\right\}. \tag{3. 58}_3$$

- ***For the cylindrical element 3*** **(fig. 3. 3)**:

$$\left\{(\sigma_1)_{3x},(\sigma_2)_{3x}\right\}=\left\{\left[(\sigma_1)_{3x}\right]_{p_i,\Delta T_3}\cdot\left(c_{i\sigma r}\right)_{3x},\ \left[(\sigma_2)_{3x}\right]_{p_i,\Delta T_3}\cdot\left(c_{i\sigma i}\right)_{3x}\right\};\quad (3.\ 59)_1$$

$$\left(c_{i\sigma r}\right)_{3x}=1+\left\{\left[\pm 6\cdot M_{3x}/\delta_3^2\right]/\left[p_i\cdot R_{m3}/(2\cdot\delta_3)+E_3\cdot\alpha_3\cdot\Delta T_3\right]\right\};\quad (3.\ 59)_2$$

$$\left(c_{i\sigma i}\right)_{3x} = 1+\left\{\left[\pm 6\cdot\mu_3\cdot M_{3x}/\delta_3^2+T_{3x}/\delta_3\right]/\left[p_i\cdot R_{m3}/\delta_3+E_3\cdot\alpha_3\cdot\Delta T_3\right]\right\}. \tag{3. 59}_3$$

Note: The plus sign in the equalities (3. 58) $_{2,3}$ and (3. 59) $_{2,3}$ is taken into account for the inner surfaces of the cylindrical components $j=1,3$ (fig. 3. 3), according to the scheme accepted for the study.

In the sense of the above, the variations of the functions M_{1x}, T_{1x}, respectively M_{3x}, T_{3x}. The sections in which these quantities are maximum are positioned, reflecting the bending stress (M_{1x}, M_{3x}), respectively the tension/compression stress in the ring direction (T_{1x}, T_{3x}). Deduct the dimensions (x_{1M} - for radial unitary momentum, unitary M_{1x} moment and x_{1T} - for annular unitary force T_{1x}); (x_{3M} - for the radial unit bending moment M_{3x} and x_{3T} - for the annular unit force T_{3x}).

3. 3. 3. 2. Equivalent voltages developed by external loads – constant

- ***For the cylindrical element 1*** **(fig. 3. 3)**:

$$\left[\left(\sigma_{ech}\right)_{1x}\right]_{p_i,\Delta T_1}=\sqrt{\begin{array}{c}\left[(\sigma_1)_{1x}\right]^2_{p_i,\Delta T_1}+\left[(\sigma_2)_{1x}\right]^2_{p_i,\Delta T_1}-\\ -\left[(\sigma_1)_{1x}\right]_{p_i,\Delta T_1}\cdot\left[(\sigma_2)_{1x}\right]_{p_i,\Delta T_1}\end{array}};\tag{3. 62}_1$$

$$\left[\left(\sigma_{ech}\right)_{1x}\right]_{p_i,\Delta T_1}=\sqrt{\begin{array}{c}3\cdot\left[p_i\cdot R_{m1}/(2\cdot\delta_1)\right]^2+\\ +3\cdot\left[p_i\cdot R_{m1}/(2\cdot\delta_1)\right]\cdot\left(E_1\cdot\alpha_1\cdot\Delta T_1\right)+\left(E_1\cdot\alpha_1\cdot\Delta T_1\right)^2\end{array}},\tag{3. 62}_2$$

or, for individual effects:

$$\left[\left(\sigma_{ech}\right)_{1x}\right]_{p_i}=\sqrt{3}\cdot p_i\cdot R_{m1}/(2\cdot\delta_1);\ \left[\left(\sigma_{ech}\right)_{1x}\right]_{\Delta T_1}=E_1\cdot\alpha_1\cdot\Delta T_1\ .\tag{3. 62}_3$$

- ***For the cylindrical element 3*** **(fig. 3.3)**:

$$\left[\left(\sigma_{ech}\right)_{3x}\right]_{p_i,\Delta T_3}=\sqrt{\begin{array}{c}\left[(\sigma_1)_{3x}\right]^2_{p_1,\Delta T_3}+\left[(\sigma_2)_{3x}\right]^2_{p_i,\Delta T_3}-\\ -\left[(\sigma_1)_{3x}\right]_{p_i,\Delta T_3}\cdot\left[(\sigma_2)_{3x}\right]_{p_i,\Delta T_3}\end{array}};\tag{3. 62}_4$$

$$\left[\left(\sigma_{ech}\right)_{3x}\right]_{p_i,\Delta T_3}=\sqrt{\begin{array}{c}3\cdot\left[p_i\cdot R_{m3}/\left(2\cdot\delta_3\right)\right]^2+\\+3\cdot\left[p_i\cdot R_{m3}/\left(2\cdot\delta_3\right)\right]\cdot\left(E_3\cdot\alpha_3\cdot\Delta T_3\right)+\left(E_3\cdot\alpha_3\cdot\Delta T_3\right)^2\end{array}},$$

(3. 62) 5

or, for individual effects:

$$\left[\left(\sigma_{ech}\right)_{3x}\right]_{p_i}=\sqrt{3}\cdot p_i\cdot R_{m3}/\left(2\cdot\delta_3\right);\left[\left(\sigma_{ech}\right)_{3x}\right]_{\Delta T_3}=E_3\cdot\alpha_3\cdot\Delta T_3. \quad (3.\ 62)\ 6$$

Equivalent voltages developed by loads connection

- ***<u>For the cylindrical element 1</u>*** **(fig. 3. 3)**:

$$\left(\sigma_{1M}\right)_{1x}=6\cdot M_{1x}/\delta_1^2;\ \left(\sigma_{2M}\right)_{1x}=\mu_1\cdot\left(\sigma_{1M}\right)_{1x};\left(\sigma_{1T}\right)_{1x}=0;\left(\sigma_{2T}\right)_{1x}=T_{1x}/\delta_1;$$

(3. 63)

The equivalent stresses existing inside or outside cylinder 1 can be evaluated with shape relations:

$$\left[\left(\sigma_{ech}\right)_{1x}\right]_{M_{1x},T_{1x}}=\sqrt{\begin{array}{c}\left(\sigma_{1M}\right)_{1x}^2+\left[\left(\sigma_{2M}\right)_{1x}+\left(\sigma_{2T}\right)_{1x}\right]^2-\\-\left(\sigma_{1M}\right)_{1x}\cdot\left[\left(\sigma_{2M}\right)_{1x}+\left(\sigma_{2T}\right)_{1x}\right]\end{array}}, \quad (3.\ 64)$$

respectively:

$$\left[\left(\sigma_{ech}\right)_{1x}\right]_{M_{1x},T_{1x}}=\sqrt{\left(1-\mu_1+\mu_1^2\right)\cdot\left(\sigma_{1M}\right)_{1x}^2+\left(2\cdot\mu_1-1\right)\cdot\left(\sigma_{1M}\right)_{1x}\cdot\left(\sigma_{2T}\right)_{1x}}. \quad (3.\ 65)$$

In case of neglect of the effect of the unit force of stretching/compressing T_{1x} , the following are reached:

$$\left[\left(\sigma_{ech}\right)_{1x}\right]_{M_{1x}}=\left(\sigma_{1M}\right)_{1x}^2\cdot\sqrt{\left(1-\mu_1+\mu_1^2\right)};\ \left[\left(\sigma_{ech}\right)_{1x}\right]_{T_{1x}}=T_{1x}/\delta_1. \quad (3.\ 66)$$

- ***<u>For the cylindrical element 3</u>*** **(fig. 3. 3)**:

$$\left(\sigma_{1M}\right)_{3x}=6\cdot M_{3x}/\delta_3^2;\ \left(\sigma_{2M}\right)_{3x}=\mu_3\cdot\left(\sigma_{1M}\right)_{3x};\left(\sigma_{1T}\right)_{3x}=0;\left(\sigma_{2T}\right)_{3x}=T_{3x}/\delta_3;$$

(3. 67)

The equivalent stresses existing inside or outside cylinder 1 can be evaluated with shape relations:

$$\left[\left(\sigma_{ech}\right)_{3x}\right]_{M_{3x},T_{3x}}=\sqrt{\begin{array}{c}\left(\sigma_{1M}\right)_{3x}^2+\left[\left(\sigma_{2M}\right)_{3x}+\left(\sigma_{2T}\right)_{3x}\right]^2-\\-\left(\sigma_{1M}\right)_{3x}\cdot\left[\left(\sigma_{2M}\right)_{3x}+\left(\sigma_{2T}\right)_{3x}\right]\end{array}}, \quad (3.\ 68)$$

respectively:

$$\left[\left(\sigma_{ech} \right)_{3x} \right]_{M_{3x}, T_{3x}} = \sqrt{ \left(1 - \mu_3 + \mu_3^2 \right) \cdot \left(\sigma_{1M} \right)_{3x}^2 + \left(2 \cdot \mu_3 - 1 \right) \cdot \left(\sigma_{1M} \right)_{3x} \cdot \left(\sigma_{2T} \right)_{3x} } . \tag{3. 69}$$

In case of neglecting the effect of the unit force of stretching/compressing, T_{3x}:

$$\left[\left(\sigma_{ech} \right)_{3x} \right]_{M_{3x}} = \left(\sigma_{1M} \right)_{3x}^2 \cdot \sqrt{ \left(1 - \mu_3 + \mu_3^2 \right) } ; \qquad \left[\left(\sigma_{ech} \right)_{1x} \right]_{T_{3x}} = T_{3x} / \delta_3 . \tag{3. 70}$$

<u>Note</u>: The equivalent stresses developed by the loads connection must be calculated in the planes where they are extreme ((76) and (77)).

Equivalent stresses (with the effect of unit shear stress)

The shear stresses developed by the unit shear forces and the unit radial bending moments, for cylindrical elements 1 and 3, can be evaluated with the relationship:

$$\left\{ \tau_{1x}, \tau_{3x} \right\} = \left\{ Q_{1x} / \delta_1 , \; Q_{3x} / \delta_3 \right\} , \tag{3. 71}$$

in which Q_{1x}, Q_{3x} and have the forms (3. 56) $_2$, (3. 57) $_2$.

When the shear effect is also taken into account, the expression of the equivalent voltage changes according to the expression **[64]:**

$$\left\{ \left(\sigma^{\bullet}_{ech} \right)_{1x} ; \left(\sigma^{\bullet}_{ech} \right)_{3x} \right\} = \left\{ \sqrt{ \left(\sigma_{ech} \right)_{1x}^2 + 3 \cdot \tau_{1x}^2 } ; \; \sqrt{ \left(\sigma_{ech} \right)_{3x}^2 + 3 \cdot \tau_{3x}^2 } \right\} , \tag{3. 72) 1}$$

respectively:

$$\left[\left(\sigma_{ech} \right)_{3x} \right]_{Q_{3x}} = \sqrt{3} \cdot \tau_{3x} . \left[\left(\sigma_{ech} \right)_{1x} \right]_{Q_{1x}} = \sqrt{3} \cdot \tau_{1x} . \tag{3. 72) 2}$$

Tensiunile echivalente totale pot fi evaluate şi prin intermediul tensiunilor echivalente parţiale ale presiunii, efectului termic, al momentelor încovoietoare radiale unitare, al forţelor unitare de întindere/comprimare, respectiv al tensiunilor de forfecare, scrise sub formele:

$$\begin{aligned} \left[\left(\sigma^{\bullet\bullet}_{ech} \right)_{1x} \right]_{max} &= c_p \cdot \left[\left(\sigma_{ech} \right)_{1x} \right]_{p_i} + c_{\Delta T} \cdot \left[\left(\sigma_{ech} \right)_{1x} \right]_{\Delta T_1} + \\ &+ c_M \cdot \left[\left(\sigma_{ech} \right)_{1x} \right]_{M_{1x}} + c_T \cdot \left[\left(\sigma_{ech} \right)_{1x} \right]_{T_{1x}} + c_Q \cdot \sqrt{3} \cdot \tau_{1x} , \end{aligned} \tag{3. 76}$$

for cylinder 1, respectively:

$$\begin{aligned} \left[\left(\sigma^{\bullet\bullet}_{ech} \right)_{3x} \right]_{max} &= c_p \cdot \left[\left(\sigma_{ech} \right)_{3x} \right]_{p_i} + c_{\Delta T} \cdot \left[\left(\sigma_{ech} \right)_{1x} \right]_{\Delta T_3} + \\ &+ c_M \cdot \left[\left(\sigma_{ech} \right)_{3x} \right]_{M_{3x}} + c_T \cdot \left[\left(\sigma_{ech} \right)_{3x} \right]_{T_{3x}} + c_Q \cdot \sqrt{3} \cdot \tau_{3x} , \end{aligned} \tag{3. 77}$$

for the cylinder 3.

In the above relations, $c_p, c_{\Delta T}, c_M, c_T, c_Q$ there are factors for selecting the effect of the specified loads: pressure, thermal gradient, unitary radial bending moment, unitary tension/compression annular stress, unitary shear stress. When the coefficients have values equal to unity, the effect of the load is present, while when the coefficients have zero values, they move away.

Note: It is necessary to evaluate the maximum values of the equivalent stresses on the surfaces of cylindrical elements 1 and 3, in order to be compared with the permissible strength characteristic of the building materials, under operating conditions. Thus, $\left\{ \left(\sigma_{ech} \right)_{1x} \right\}_{max} \leq \sigma_{1a} = c_s \cdot \sigma_c$ or $\left\{ \left(\sigma_{ech} \right)_{3x} \right\}_{max} \leq \sigma_{3a} = c_s \cdot \sigma_c$, σ_c representing the conventional flow limit of the metallic material.

►▼◄

Resorting to ***the criterion of participation or contribution of the loads*** regarding the load-bearing capacity of the analyzed structure, it can be written:

$$\left[f_{pp} \right]_j + \left[f_{p\Delta T} \right]_j + \left[f_{pM_x} \right]_j + \left[f_{pT_x} \right]_j + \left[f_{p\tau_x} \right]_j \leq 1, \qquad (3.\ 78)$$

where the notations were used: f_{pp} − the participation/contribution factor corresponding to the working pressure; $f_{p\Delta T}$ - the factor of participation/contribution of the thermal effect; f_{pM_x} - the participation/contribution factor of the unitary radial bending moment, with maximum value, at a current elevation x, located along the length of the cylindrical envelope; f_{pT_x} - the participation/contribution factor of the annular unit force of tension/compression, at a current level x, located along the analyzed cylindrical shell; $f_{p\tau_x}$ - the participation/contribution factor of the cutting unit force, at a current elevation x, measured along the cylindrical shell; j − represents the number of the cylindrical shell considered.

3. 3. 4. Conclusions

In the foregoing, the analysis of the stress states developed in a structure consisting of a flat plate with a central hole and a connecting tube, respectively a cylinder that is welded to the marginal part of the plate, is considered. It is considered a relatively small plate, so the effects of marginal loads are felt mutually. Cylindrical elements are appreciated as long. The materials from which the components of the structure are made can be the same or different. The mathematical expressions deduced for both the linking tasks and for the work tasks, value constants.

C H A P T E R 4

Experimental analysis of stress states in areas with structural discontinuities of technological equipment, using the electrotensometric method

4. 1. Introduction

In the current state of knowledge, it is mentioned that the technology of manufacturing the component elements intended to be incorporated into a pressure equipment has an important role in the appearance and development of defects **[1, 2].** In this context, this paper proposes to make contributions regarding the issue of the influence of geometric defects and discontinuities on the bearing capacity of technological systems under pressure.

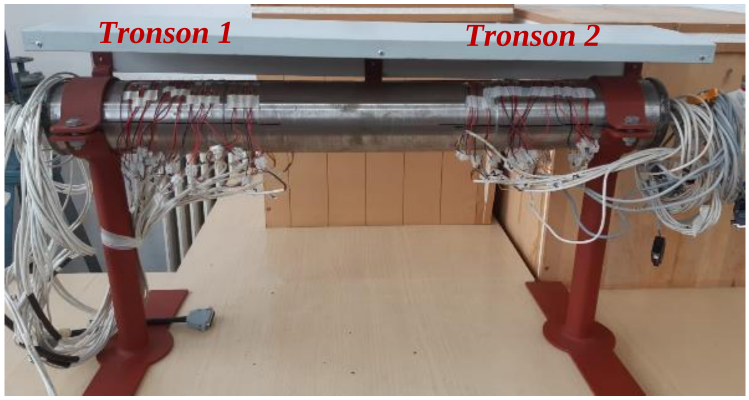

Fig. 4. 8. Experimental model

4. 2. Experimental study on a model with geometric discontinuities

4. 2. 1. Purpose of experimental research

The study presents the experimental results obtained from the tests carried out on a cylindrical body with variable geometry, stressed at an internal pressure in three stages. The case of a transition without connection from a wall thickness to a lower thickness of the cylindrical body (or vice versa) is discussed, in which case the values of the specific linear deformations and the corresponding stresses are established experimentally. In this case, electro-resistive blood pressure was used.

4. 2. 2. Object of experimental research

The present study aims to determine the stresses manifested on the cylindrical outer surface of areas with different geometries, using the electro-resistive tensometry method.

4. 2. 3. Methodology of experimental research

Electroresistive tensometry is an effective method for the practical verification of the state of mechanical stresses in the situation of a technical system, which is difficult to analyze by analytical procedures, because it allows the measurement of specific linear deformations in several directions and the application of analytical formulas corresponding to the theory of elasticity **[33 - 35].**

In order to carry out the research approached in the present case, a model was developed for conducting experiments (fig. 4. 2).

a)

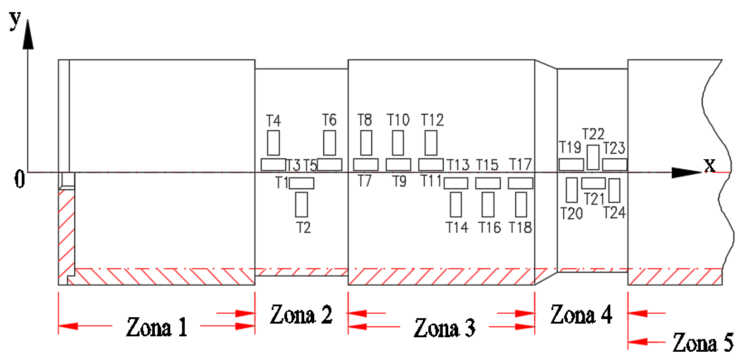

b)

Fig. 4. 6. Experimental model - Section 1
(a) section 1; b) sketch 1 – location of transducers 1, 2, 3 ... 24.

3.

The construction material of the experimental model is P265GH, with the symbolization 1.0425, according to EN 10216 (yield strength, $Rp_{0,2} = 265\ \mathrm{N/mm^2}$ tensile strength, $R_m = 410 - 570\ \mathrm{N/mm^2}$ tensile length, $A = 32\,\%$).

The other characteristics of the experimental model are presented as: pipe dimensions (diameter x length x thickness) Ø114.3 mm x 931 mm x8 mm; cover (diameter x thickness) Ø114.3 x 10 mm, 2 pcs.; pipe supports, 2 pcs.; equipment protection made of sheet metal with a thickness of 1mm; 2 connections $2^{1/2}$"; supply valve $2^{1/2}$"; Afriso pressure gauge, p_{max} = 4 MPa.

Transducers were placed on the experimental model as shown in **figures 4. 6** and **4. 7.**

The model was divided into two sections, namely section 1 (left side – with pressure gauge) and section 2 (right side – with power connection). The model has been divided into 9 zones. Zones 1, 5 and 9 were areas of constant thickness, on which no transducers were placed and which, in the present work, were not taken into account for research. Zones 2 (50 mm in size), 3 (100 mm in size), 4 (50 mm in size), 6 (50 mm in size), 7 (100 mm in size) and 8 (50 mm in size), are areas of different thicknesses and different diameter passages, where transducers have been placed, as follows:

- Zone 2, with the T1... T6 transducers, the outer diameter of the pipe $\phi 109\ mm$.
- Zone 3, with the T7... T18 transducers, the outer diameter of the pipe $\phi 113{,}5\ mm$.
- Zone 4, with the T19... T24 transducers, the outer diameter of the pipe $\phi 109{,}5\ mm$.
- Zone 6, with the T25... T30 transducers, the outer diameter of the pipe $\phi 108{,}5\ mm$.
- Zone 7, with the T31... T42 transducers, the outer diameter of the pipe $\phi 113{,}5\ mm$.

- Zone 8, with T43 transducers... T48, the outer diameter of the pipe $\phi 108,5\ mm$.

a)

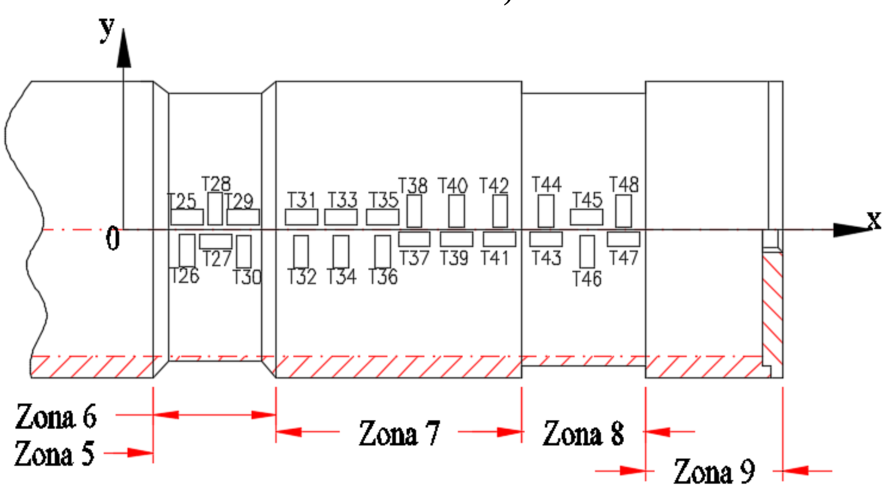

b)

Fig. 4. 7. Model experimental - Section 2

a) Section 2; b) sketch 2 – location of transducers 25, 26, 27....48.

The calculation of the stresses, on each area of the experimental model, depending on the internal pressure, was performed with the formulas from **[33 - 35],** corresponding to the cylindrical rotation shells.

4. 2. 4. Equipment used for experimental research

To carry out the experiments, the following equipment was used, as well as the software for testing:

1. Experimental stand (**fig. 4. 9**)
2. Pressure gauge pump (**fig. 4. 11**).
3. MGCplus equipments (**fig. 4. 12**), required for data acquisition (MGCplus 1 purchased 40 measuring points and MGCplus 2 purchased 8 measuring points).
4. Lenovo laptop (**fig. 4. 13**) with Catman Easy software, required for experimental data acquisition.

5. Strain gauge transducers with film type 6/120 LY 11, manufactured by the Hottinger company; single direction (L) according to the code, polyamide resin support (Y), measuring base 6 mm, strength 120 Ω ±0.2%, thermal coefficient α = 11·10-6 , K-1 (for steel), plus data in the leaflet; k and the temperature range, between -70°C and +200°C.

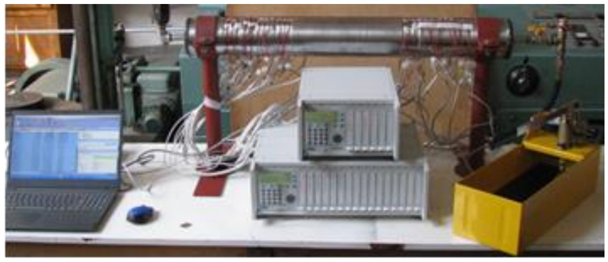

Fig. 4. 9. Experimental stand

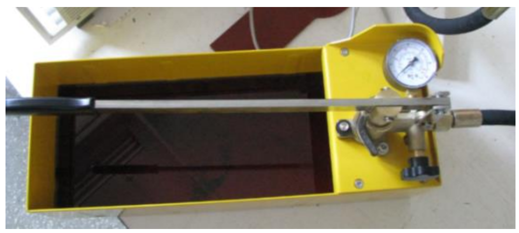

Fig. 4. 11. Pressure gauge pump

Fig. 4. 12. MGCplus 1 and MGCplus 2 equipments

Fig. 4. 13. Lenovo laptop with Catman Easy software

4. 2. 5. Experimental research

During the experimental research, the following cases were considered:

1. In case 1, an internal pressure was used in the equipment up to the value $p_1 = 1$ [MPa] = 1 [N/mm ^{2}], after which it was unloaded up to the value 0 [MPa] = 0 [N/mm ^{2}].

2. In case 2, an internal pressure was used in the equipment up to the value $p_2 = 2$ [MPa] = 2 [N/mm ^{2}] after which, it was discharged up to the value 0 [MPa] = 0 [N/mm ^{2}].

3. In case 3, an internal pressure was raised in the equipment to the value p 3 = 3 [MPa] = 3 [N/mm ^{2}], after which it was discharged to the value 0 [MPa] = 0 [N/mm ^{2}].

With the help of MGCplus, the specific linear deformations on the radial direction and on the annular direction were obtained, at the ascent/descent pressures, mentioned above.

4. 2. 6. Results of experimental research

The values of the theoretical equivalent stresses, $\sigma_{ech\,t}$ calculated with the formula (4.6) and the relations (4.1), respectively, over the length of section 1 (areas 2, 3 and 4) and over the length of section 2 (areas 6, 7 and 8), are shown in Table 4.1:

Table 4. 1. Results of theoretical equivalent stress calculated in the 6 zones

Pressure [MPa]	**Zone 2**	**Zone 3**	**Zone 4**	**Zone 6**	**Zone 7**	**Zone 8**
	$\sigma_{ech\,t}$ **[MPa]**					
$p_1 = 1$	8.39	6.03	8.03	8.78	8.99	5.89
$p_2 = 2$	16.78	12.07	16.07	17.56	17.98	11.78
$p_3 = 3$	25.17	18.10	24.10	26.34	26.97	17.67

The theoretical equivalent stresses, calculated over the length of each section, without concentrations influenced by discontinuities, are used to compare with the values of the experimental equivalent stresses, in the different sections mentioned in **figures 4. 14 – 4. 19**.

4. 2. 7. Processing and interpretation of results

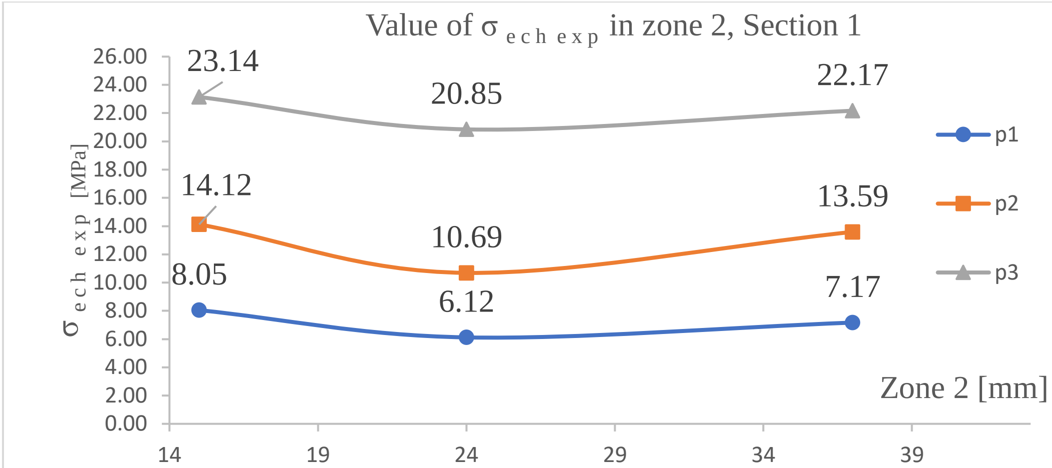

Fig. 4. 14. Values of experimental equivalent stresses in zone 2, Section 1

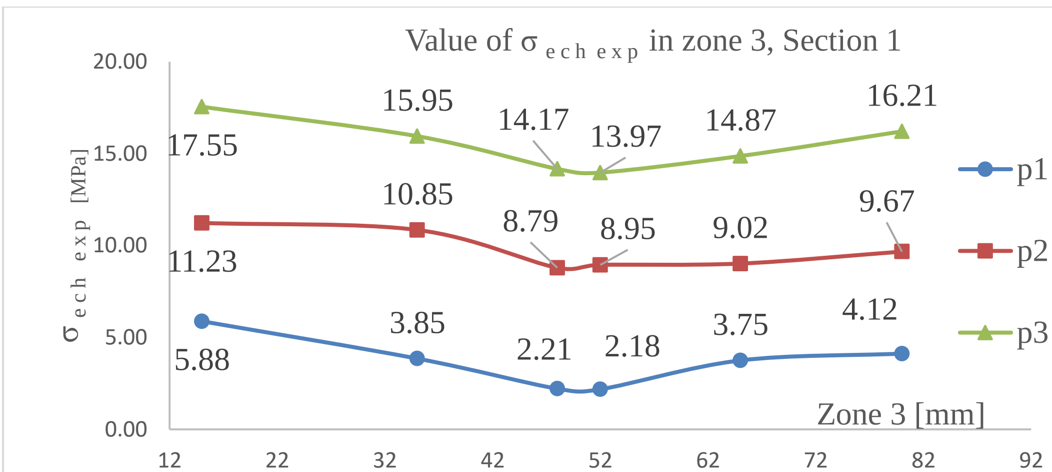

Fig. 4. 15. Values of experimental equivalent stresses in Zone 3, Section 1

Figures 4.14 – 4.19 show the variations of the experimental equivalent stress, $\sigma_{ech\,exp}$ calculated with the formula (4.6), on the length of Section 1 (zones 2, 3 and 4) and on the length of Section 2 (zones 6, 7 and 8) – in sections with transducers.

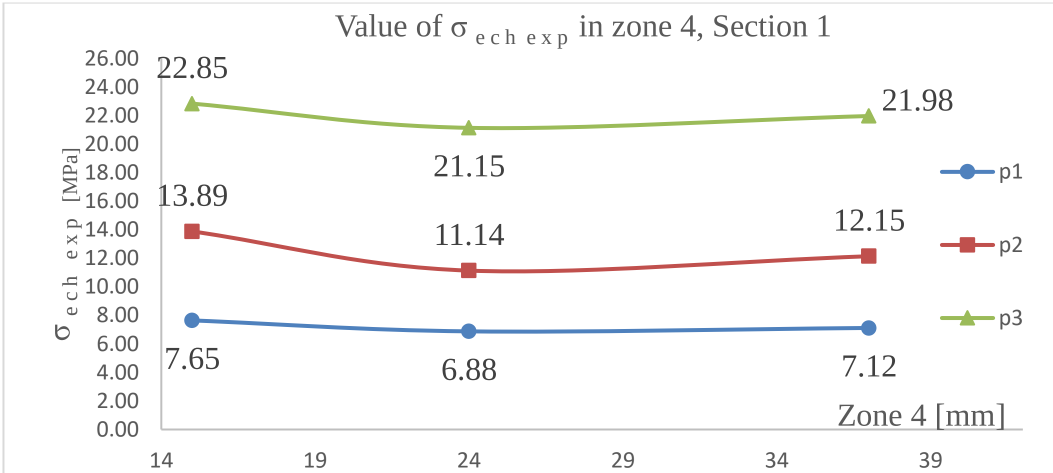

Fig. 4. 16. Values of experimental equivalent stresses in Zone 4, Section 1

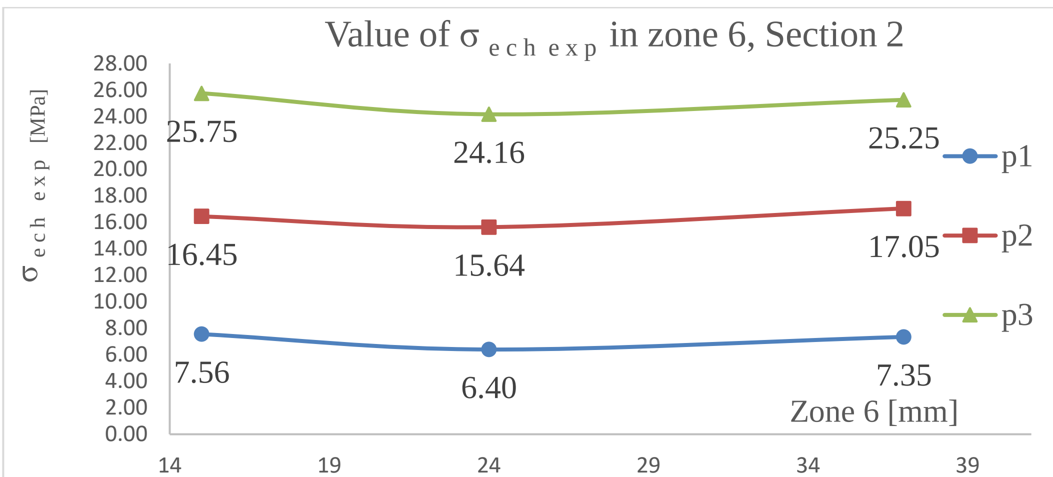

Fig. 4. 17. Experimental equivalent stress values in Zone 6, Section 2

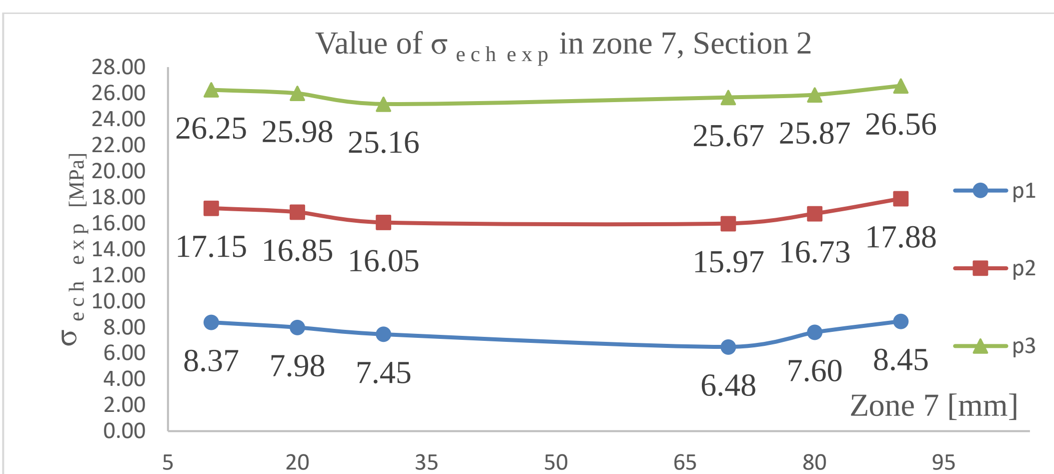

Fig. 4. 18. Values of experimental equivalent stresses in Zone 7, Section 2

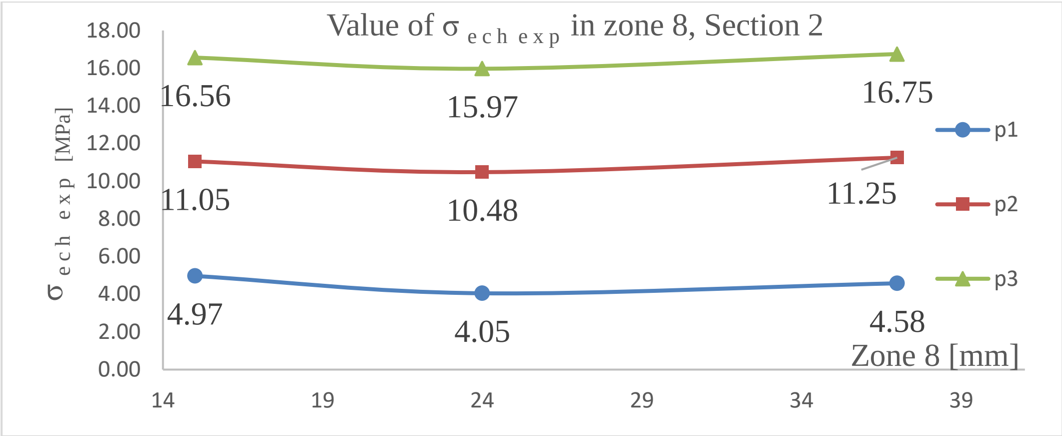

Fig. 4. 19. Values of experimental equivalent stresses in Zone 8, Section 2

It is observed that for all the analyzed areas, the values of the measured equivalent voltages are lower than the values of the theoretical equivalent voltages. For example, in zone 7, for pressure $p_2 = 3\,MPa$, there are:

$$\sigma_{ech\,exp} = 25,92\,MPa \quad < \quad \sigma_{ech\ t} = 26,97\,MPa\,.$$

The experiment was considered to have taken place under normal working conditions and at ambient temperature.

4. 2. 8. Conclusions

From the interpretation of the results obtained, it can be seen that an increase in the internal pressure produces an adequate change in the radial and annular stresses, respectively in the equivalent stresses.

It is noted that the experimental equivalent stresses are lower, in value, than the equivalent membrane voltages. The differences are insignificant in the experiment performed.

4. 3. Experimental study on a model with a fault channel type

On the left side of the experimental model (**fig. 4. 21**), currently, at a distance of 70 mm from the left end, a channel of the same size was built $\phi 5\ mm$ x $50\ mm$ – and a connection with a tap was installed. On the right side (**fig. 4. 22**), at a distance of 70 mm, a channel of the size was built $\phi 3\ mm$ x $30\ mm$ – and a connection with a pressure gauge was installed.

a) Channel 1

b) Channel 1 dimensions

c) Connection and supply valve

Fig. 4. 21. Left side of the experimental model

a) Canalul 2

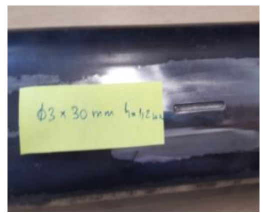

b) Dimensiunile canalului 2

c) Racord și manometru

Fig. 4. 22. Partea dreaptă a modelului experimental

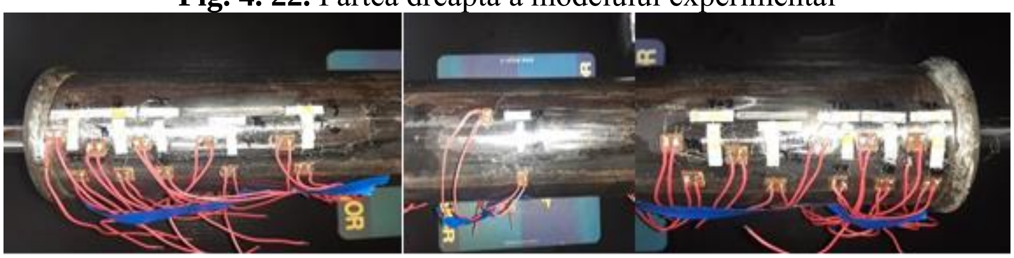

Fig. 4. 24. Amplasare traductori pe modelul experimental

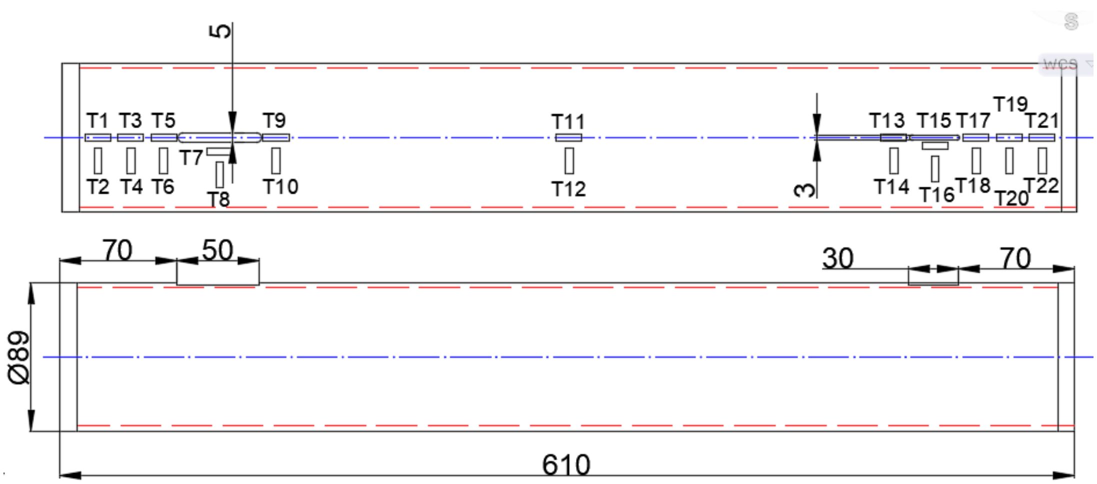

Fig. 4. 25. Tensometric transducer location sketch

Tensometric transducers were placed on the experimental model, starting with the numbering on the left side, according to **figures 4. 24 and 4.25**.

During the experiments, the following cases were considered:

1. In case 1, an internal pressure was used in the equipment up to the value $p_1 = 1$ [MPa], after which it was unloaded up to the value 0 MPa.

2. In case 2, an internal pressure was used in the equipment up to the value $p_2 = 2$ [MPa], after which it was discharged up to the value 0 MPa.

3. In case 3, an internal pressure was raised in the equipment up to the value $p_3 = 3$ [MPa], after which it was discharged up to the value 0 MPa.

With the help of the MGCplus tensor bridge, the specific linear deformations in the radial direction and in the ring direction were obtained at the pressures mentioned above.

The calculation of the stresses on each area of the experimental model, depending on the internal pressure, was performed with the known formulas.

4. 3. 1. Equipment used for experimental research

The composition of the equipment used for experimentation is the one described in the case 4. 2.

It is worth mentioning that only the transducers located around the 2 channels were taken into account for the analysis, respectively transducers 5, 6, ... 10 and 13, 14, ... 18 (fig. 4. 22).

It is observed that for the areas around the 2 channels, after being filled with a composite material, the values of the measured equivalent stresses are lower than the values of the equivalent stresses measured initially, in the areas adjacent to the channel.

The experiment was considered to have taken place under normal working conditions and at ambient temperature.

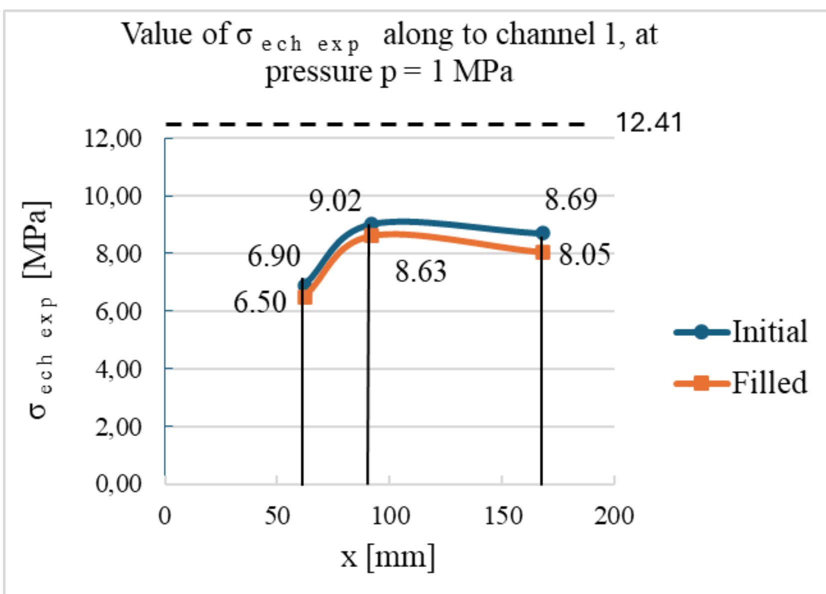

Fig. 4. 32. The values of the experimental equivalent stress, along to channel 1, for pressure p=1 MPa

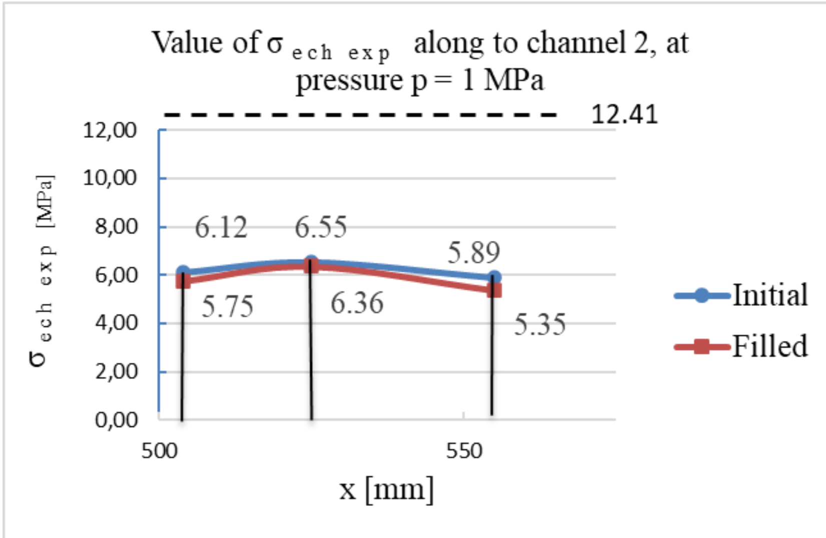

Fig. 4. 33. The values of the experimental equivalent stress, along to channel 2, for pressure p=1 MPa

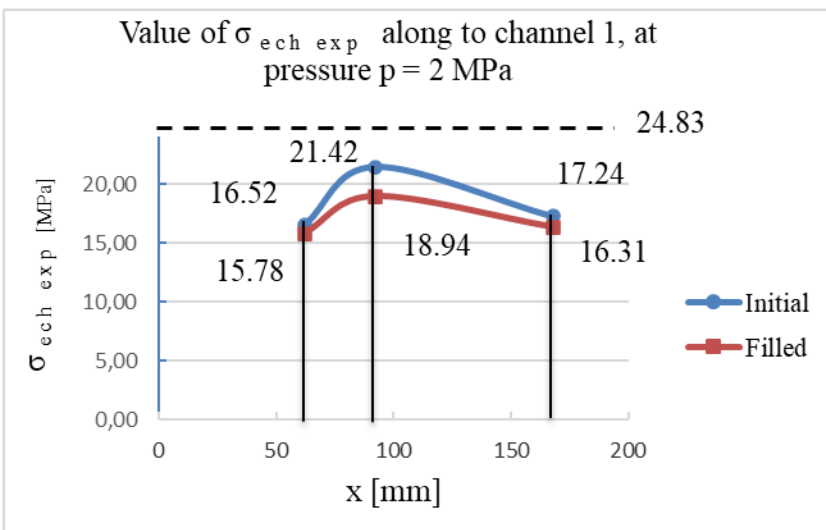

Fig. 4. 34. The values of the experimental equivalent stress, along to channel 1, for pressure p=2 MPa

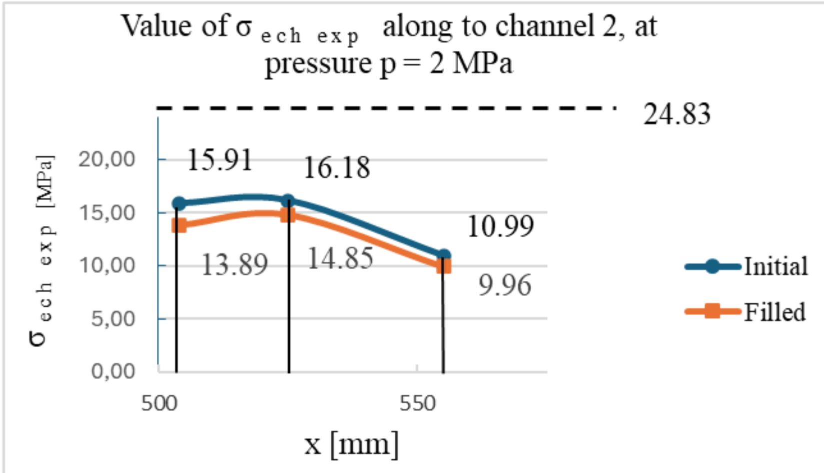

Fig. 4. 35. The values of the experimental equivalent stress, along to channel 2, for pressure p=2 MPa

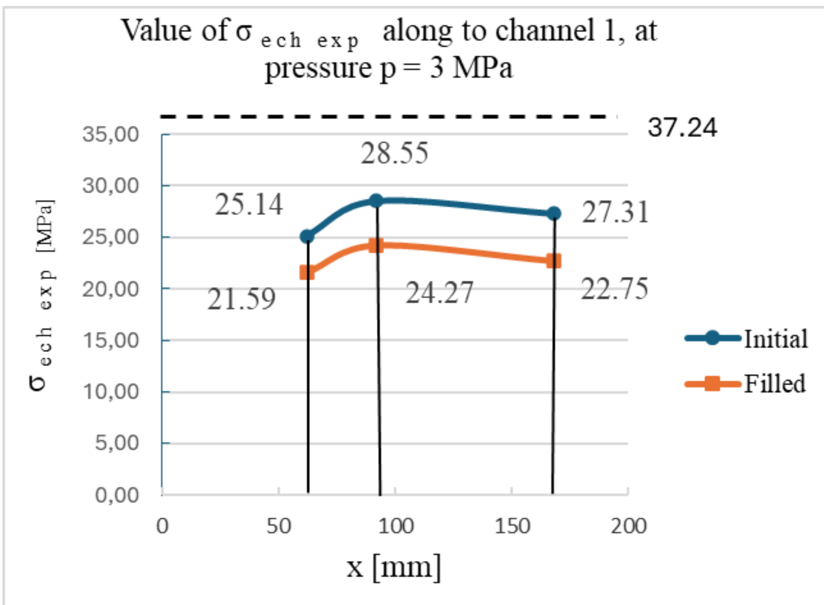

Fig. 4. 36. The values of the experimental equivalent stress, along to channel 1, for pressure p=3 MPa

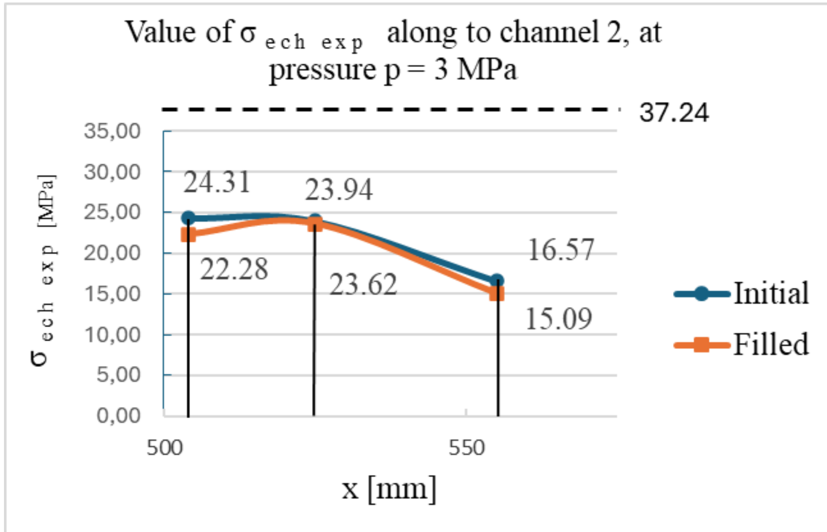

Fig. 4. 37. The values of the experimental equivalent stress, along to channel 2, for pressure p=3 MPa

4. 4. Conclusions

It is noted that the experimental equivalent stresses are lower, in value, than the equivalent membrane stress. The differences are insignificant in the experiment performed.

A closer analysis confirms the higher values of specific linear deformations, developed in the annular (circumferential) direction, which illustrates a "***possible splitting effect***".

CHAPTER 5

Analysis of stress states in areas with geometric discontinuities of technological equipment, using the finite element method

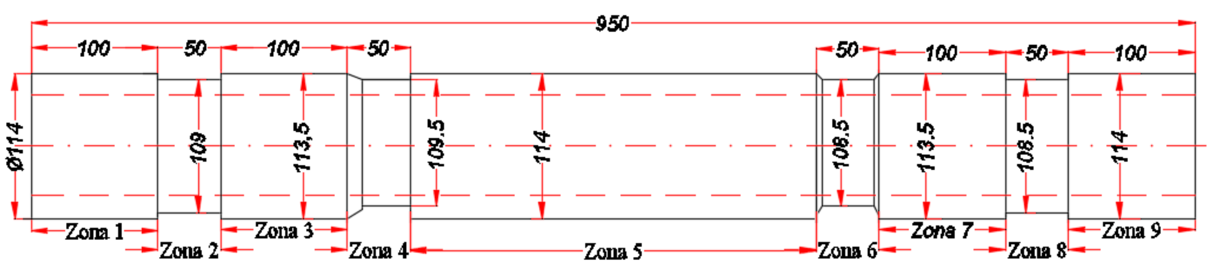

a)

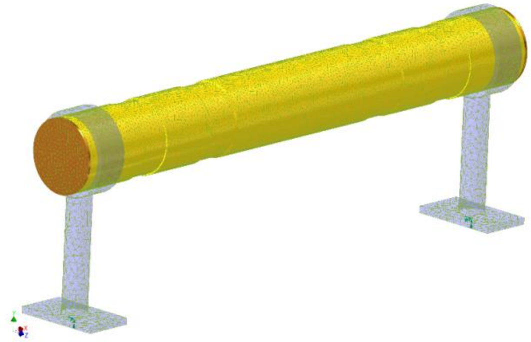

b)

Fig. 5. 1. The geometric model **-** a) the sketch of the model; **-** b) the geometric model built in Inventor software

5. 1. Introduction

Finite element modeling is currently widely used in academia and industry. The applications used to support the design and strength assessment of various mechanical structures are a basis for their safe operation **[24 - 26].** Analysis by this method is an integral and major component in many fields of engineering design and manufacturing.

5. 2. Numerical research on geometric model 1

The purpose of the study is the numerical analysis with the finite element method (FEM) performed on a cylindrical body with variable geometry, stressed at an internal pressure. The case of a transition without connection from a wall thickness to a lower one is discussed, in which case the values of the specific linear deformations and the corresponding stresses are investigated. For this purpose, a geometric model built in Inventor Professional was made and then imported into Nastran In-CAD for the MEF calculation of the object.

5. 2. 1. Numerical research with *NASTRAN software*

The discretization of the geometric model was done with solid elements, according to the tetrahedral method, with parabolic sides for the pipe and linear for the rest of the components, with the dimensions shown in figure 5. 2.

	Part Name	*Visibility*	*Color*	*Size (mm)*	*Tolerance (mm)*	*Element Order*	*Settings*	*Nodes*	*Elements*
	Ansamblu 2.i...	☑		38,4778	0,000769555	Parabolic	Settings	0	0
	Capac_24.03....	☑		6,05416	0,000121083	Linear	Settings	4421	2327
	Capac_24.03....	☑		6,05416	0,000121083	Linear	Settings	753	2478
	Model_rev.1:1	☑		5,5	0,00072112	Parabolic	Settings	171203	98631
	Suport:1	☑		13,2618	0,000265237	Linear	Settings	725	2216
	Suport:2	☑		13,2618	0,000265237	Linear	Settings	711	2143

Fig. 5. 2. Geometric model discretization

The load is given by the internal pressure, $p = 3MPa$, and the condition of ensuring a convergence of the results has been imposed $< 2\%$. This requirement allows for the automation of the discretized network refinement process during the evaluation process. In this case, a 5-step global refinement was required, which will allow the size of the finished element to be changed over the entire volume of the piece.

The **von Mises** equivalent stresses (calculated on the basis of the main stresses) obtained using the MEF, in different sections, show a maximum of $48,61\ MPa$ in the cap area, but on the pipe stresses are obtained $< 24\ MPa$ in the areas of lower thickness and around $15\ MPa$ in the areas of greater thickness (**fig. 5. 4**).

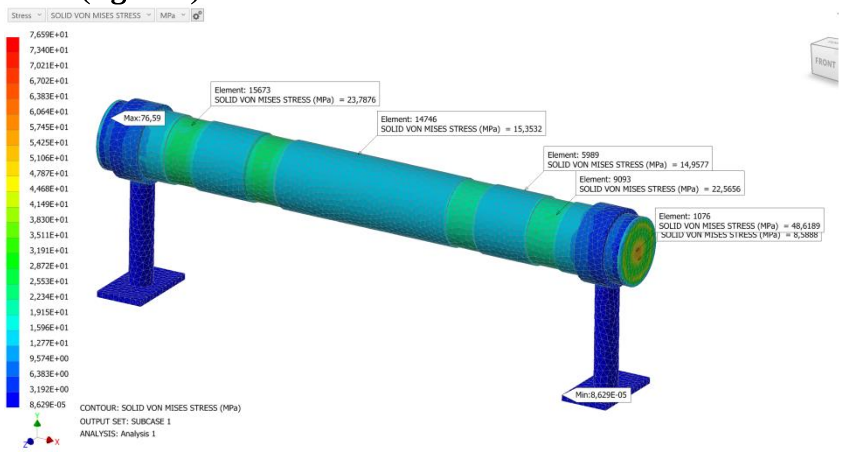

Fig. 5. 4. Values of the equivalent stresses in relation to the internal pressure, $p = 3\ MPa$

5. 2. 2. Numerical research with *ANSYS software*

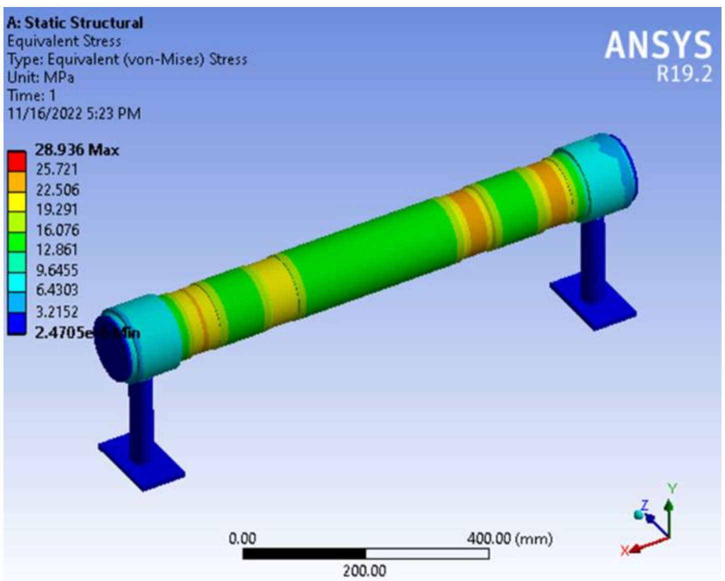

Fig. 5. 12. Values of equivalent stress

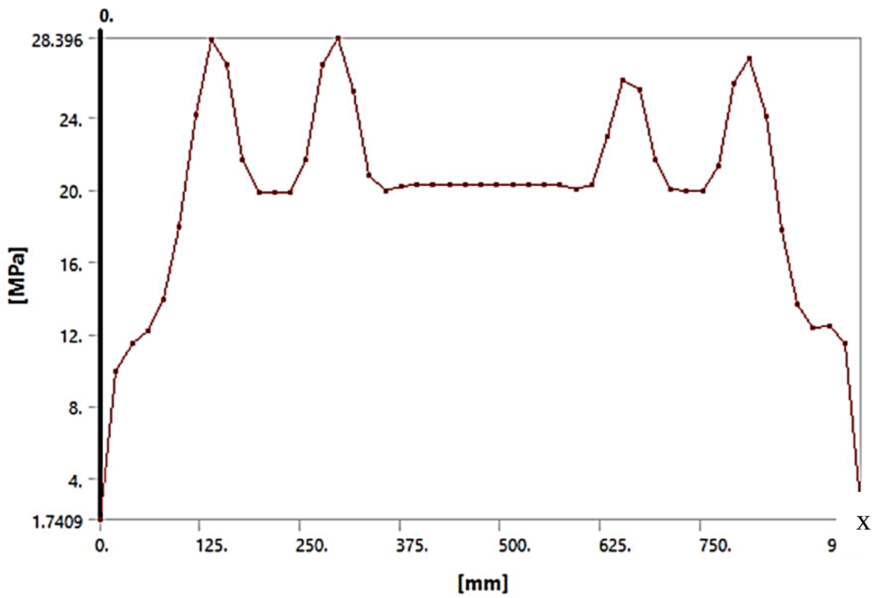

Fig. 5. 14. Values of the equivalent stress at the points located on the outdoor generator

Conclusions

The results of the calculations through the two simulation programs lead to similar results. For example, the maximum equivalent contour stress obtained was from $23,86\,MPa$ modeling with Nastran software and from $28,39\,MPa$ modeling with Ansys software.

5. 3. Numerical research on geometric model 2

The load is given by the internal pressure, $p = 3MPa$, and the condition of ensuring a convergence of the results has been imposed $< 2\%$.

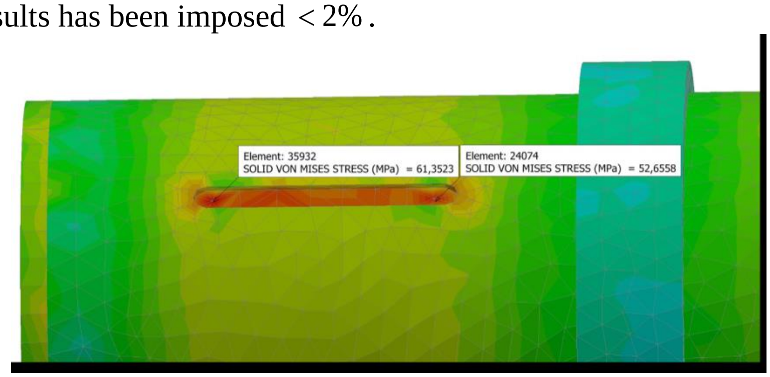

Fig. 5. 17. Values of von Mises stresses along to channel 1.

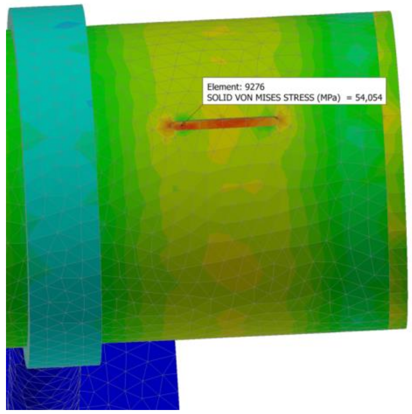

Fig. 5. 18. Value of von Mises stresses along to channel 2

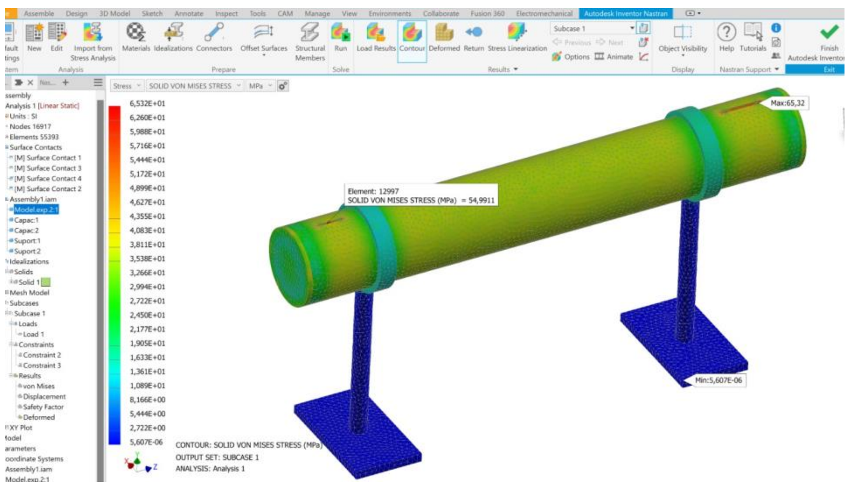

Fig. 5. 19. Maximum stress values for 2 channels.

The values obtained by the Nastran numerical method show a maximum of $65{,}32MPa$ for channel 1 and a maximum of for $54{,}99MPa$ channel 2, indicating that in those areas the equivalent stresses are maximum and can influence the further development of defects.

The presented geometric model can be the basis for further analysis, it is suggested to use the so-called hybrid approach, combining the analytical and experimental method with finite element modeling. This allows the identification of the state of stresses and deformations during dynamic loads and at any chosen point of the structure, especially since *the generation of stresses can influence the integrity of the structure* **[31].**

5. 4. Conclusions

The geometric models presented in this chapter are experimental models, have the characteristics described in chapter 4 and were modeled using the Inventor Professional software and then imported into Nastran In-CAD and Ansys for the MEF calculation.

The numerical results obtained with the help of MEF modelling validated the experimental results in chapter 4.

C H A P T E R 6

CONCLUSIONS. OWN CONTRIBUTIONS. PERSPECTIVES

6. 1. Conclusions

The permanent development of mankind has permanently imposed industrial development, for the production of diversified products and in increasing quantities. As a natural consequence, there was a transition to increasingly complicated and high-performance constructions for the processing of raw materials, but also other substitute materials. In this sense, the orientation towards secondary materials resulting from industrial processes has been developed, in order to reduce the recognized raw materials, whose quantities are decreasing. Composite materials have found an increasingly obvious application.

Industrial equipment has obtained increasingly complicated configurations that have required the development of adequate calculation methods, with the imposition of the advantage of computers. We gradually moved on to intimate analyses of the constructions. This category also includes geometric discontinuities, with sudden passage from one shape to another, or with connection or linear passage. In the sense of the above, the theme of this thesis is also inscribed.

Obviously, the stages that can be noted from design to manufacturing, transport, commissioning and operation in operation were also discussed.

- Some aspects related to the transport of oversized equipment are analyzed by the specialized literature, situations when unwanted deformations may occur, in the longitudinal direction of the cylindrical surfaces or deformations of the cross-sections, developed by the unevenness of the routes, for example.
- Another type of industrial structure is the technological pipes, above ground or buried. In this situation, the effect produced by internal corrosion or external corrosion of pipes is noticeable. In this regard, the analysis is very important to detect the effect of corrosion on the thickness of the walls. The appearance of surface defects or cracks and the development of breakage are not neglected.
- The deviations in the shape of the surfaces that can be found on the components of the mechanical structures under pressure, regardless of their geometry, can be deviations from: a) the given shape of the surface; circularity; cylindricity; the given shape of the profile; straightness; flatness.
- Aspects regarding the evaluation of the service life. The example is made in the case of two ferrules with offset median surfaces, respectively in the case of pipes with specific defects.

6. 2. Own contributions

Within the theme adopted for the doctoral thesis, the following were considered:

Theoretical aspects

a) Analytical study of stress states in cylindrical areas with geometric discontinuities, including: study hypotheses; establishing liaison tasks; states of tension; Conclusions.

b) Analytical study of stress states in a flat circular plate and a central connection, including: study assumptions; strain continuity equations; bond loads; stress states; conclusions.

c) Analysis of stress states in areas with geometric discontinuities of technological equipment, using the finite element method, including: numerical research on geometric model 1 (numerical research with *NASTRAN software*; numerical research with *ANSYS software*); numerical research on geometric model 2 (numerical research with *NASTRAN software)*; conclusions.

Experimental aspects

Experimental analysis of stress states in areas with structural discontinuities of technological equipment, using the electrotensometric method, including:

- Experimental study on a model with geometric discontinuities (purpose of experimental research; object of experimental research; method of experimental research; equipment used for experimental research; conduct of experimental research; the results of experimental research; processing and interpretation of results; cxoncluses).
- Experimental study on a model with a wedge channel defect (equipment used for experimental research; experimental results obtained; conclusions).

6. 3. Perspectives

For future research, the following are proposed:

- Analysis of stress states developed in areas with structural discontinuities between cylindrical, truncated-conical or domed shapes, during the design phase or during the operation of equipment where specific defects have been found. The following shall be used for this purpose: a) *the short cylindrical element method*; b) *the lamellar element method*.
- Development of the finite element method, in structures analyzed during the exploitation period.
- Development of experiments in structures in the testing or exploitation phase.